

New Standard Magnetic Observation System of Kakioka (KASMMER)

By

**KAZUO YANAGIHARA, MAKOTO KAWAMURA,
YUKIZO SANO and TADA0 KUBOKI**

Kakioka Magnetic Observatory

Abstract:—A new system, which is called KASMMER (Kakioka Automatic Standard Magnetometer), has been constructed for the standard magnetic observation at Kakioka. The main equipment consists of four optical pumping magnetometers, a proton magnetometer, the DI-72 (newly designed magnetometer theodolite for the absolute value determination of the declination and the dip) and a computer system. The whole system is operated automatically except the DI-72. Digital data of the geomagnetic field is obtained with an absolute accuracy of 0.1γ and with the least possible delay.

Four optical pumping magnetometers can give the finest possible time resolution for each component of the geomagnetic field at the present, though minute-values only are utilized for the primary data processing in routine operation, and also make it possible to compare the measured value of a component with the calculated one from the other components in order to watch the operation or to check the preciseness of the instruments. The ASMO method proposed by Alldredge also can be utilized when any of the optical pumping magnetometers meets trouble. Instrumental parameter of the optical pumping magnetometer is calibrated by the proton magnetometer and the DI-72. The DI-72 determines the declination and the dip with an absolute accuracy of $1''$. A vector proton magnetometer MO-P installed in 1963 supplements calibration measurements.

All data is processed in the computer system comprising two mini-computers and many accessories. The processed data is stored initially in the magnetic disc memory and then filed in the digital magnetic tape. A curve follower and a curve plotter facilitate the analog-to-digital and digital-to-analog conversion of internal and external data.

Test operations for a few months have given satisfactory results.

CONTENTS

Chapter 1. Introduction	218
1.1 Magnetic observation at Kakioka	218
1.2 Design of a new system for standard magnetic observation at Kakioka.....	221

Chapter 2. Instruments of the KASMMER System.....	223
2.1 Outline	223
2.2 Optical pumping magnetometer	226
2.3 Helmholtz coil pairs of the optical pumping magnetometer.....	232
2.4 <i>D</i> measurement	233
2.5 ASMO system.....	234
2.6 Proton magnetometer	235
2.7 DI-72	236
2.8 Large coil system.....	243
2.9 Data acquisition system.....	244
Chapter 3. Observation Houses	246
3.1 General layout of the ground and houses for the KASMMER	246
3.2 Arrangement of sensor houses.....	249
3.3 Sensor houses for the optical pumping magnetometer	251
3.4 Calibration house 1	253
3.5 Other houses	254
3.6 Magnetic survey	256
Chapter 4. Operation and Test Result	258
4.1 Present state of KASMMER operation	258
4.2 Primary data processing for continuous operation of the optical pumping magnetometers.....	258
4.3 Accuracy of the optical pumping magnetometer and continuous operation of the proton magnetometer.....	262
4.4 Calibration measurement	266
4.5 ASMO method.....	270
4.6 Semi-automatic digitization of analog record and reproduction of magnetogram from digital data	272
Appendix.....	273

Chapter 1. Introduction

1.1 Magnetic observation at Kakioka

Kakioka Magnetic Observatory ($36^{\circ}14'N$, $140^{\circ}11'E$) was established as the successor to the Tokyo Observatory ($35^{\circ}41'N$, $139^{\circ}45'E$) at the end of 1912 when rapid increase of artificial disturbance in the magnetic field was considered to be inevitable in the big city Tokyo. Since January 1, 1913, continuous magnetic observations have been carried out at Kakioka.

The observatory stands on a foot of a small hill in the outskirts of a small town, Kakioka which is situated in a hilly region approximately 72 km NE of Tokyo (Fig. 1). Surrounding low mountains, called the Tsukuba Mountains, consist mainly of granitic rocks. The highest peak is Mt. Tsukuba (876 m). A low basin extends to the east of the highest peak, and Kakioka is located near its center.

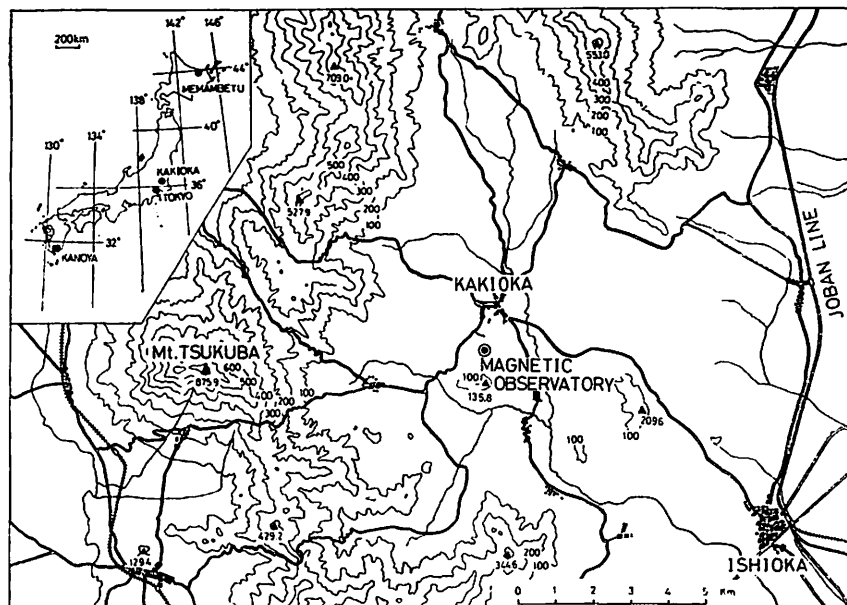


Fig. 1. Map showing the situation of the Kakioka Magnetic Observatory.

Outcrops of granitic rock are scattered in the superficial layers of approximately 100 m thick near the observatory.

To the east of the observatory the electric railway Joban Line of Japan National Railway runs from north to south. The shortest distance is approximately 10 km. However it causes no disturbance on magnetogram because an AC power is used for the line. Other local lines use Diesel engine or gasoline engine cars. Though DC power is used for railway lines near Tokyo, its disturbances at Kakioka are estimated at 0.1γ or less. Other possible sources of artificial disturbance, such as heavy industrial activities or heavy road traffic, are not found around the observatory.

At the beginning of the magnetic observation at Kakioka, a Wild-Edelmann magnetic theodolite and an earth-inductor were employed for the base-line value determination (absolute measurement), together with an Eschenhagen magnetograph for the variation measurement. A set of a Schmidt normal theodolite, an earth-inductor and a variograph made by Askania Werke was added 10 years later.

Since 1947 many investigations have been carried out on instrument improvement by the observatory staffs, and the improved instruments made in the observatory factory or industrial makers in Japan have replaced the former ones.

The variometer now used for horizontal component H or declination D is a

unifilar type in principle like the Eschenhagen or Schmidt variometers, however improved devices facilitate keeping of good stability. For example, the suspended magnet of the variometer is shunted by a small alloy so as to compensate for temperature change (Kuboki, 1968).

The vertical force variometer is a thread suspension type improved from the one proposed by Watson (1926). A small bar magnet is hung by two nearly horizontal quartz fibers from right and left. The end of one quartz fiber is welded with a small quartz spring. A shunt alloy is used also for temperature compensation. The schematic sections of the variometers are shown in Figs. A1 and A2 of the Appendix. The theory and experimental results have been reported by Kuboki (1968).

For the absolute measurement, a universal standard magnetometer and a sine galvanometer were installed in 1956. Universal standard magnetometer A-56 has a Helmholtz coil of about 20 cm in diameter whose dimensions have been determined with a precision of 1μ . Therefore, it can create a known magnetic field at the center in any given direction by turning round the vertical and horizontal axes. A search coil at the center finds the direction of the total magnetic field which is the vector sum of the geomagnetic field and the added field. The geomagnetic field can be calculated from combination of a few measurements under different fields of the Helmholtz coil. The sine galvanometer H-56 employs a similar Helmholtz coil. The absolute accuracy of the A-56 and the H-56 is estimated at 0.5γ for horizontal component H , vertical component Z and total force F and $3''$ for declination D and inclination I . These magnetometers have been in operation since 1958.

A vector proton magnetometer (the MO-P) capable of measuring H and Z with an accuracy of 0.2γ (see Appendix) together with F was added in 1963 to determine the base-line value. Now the routine determination (once a week) of base-line values is performed by the MO-P for H and Z and by the A-56 for D .

Hourly values or any instantaneous values are hand-scaled on magnetogram. Their accuracy must be less than those of the absolute measurement such as 0.2γ or so because of errors due to hand-scaling or base-line stability. On the other hand recent development of the earth sciences demands more accuracy in the measurement of geomagnetic field. For example, very small changes in geomagnetic field are investigated with special reference to earthquake prediction researches. Quick supply of data in a computer readable form is another urgent request to magnetic observatories. The observation system of traditional type needs much time and observer's labour for it.

Kakioka Magnetic Observatory had planned since 1968 to establish a new system of such magnetic observation that produces more accurate geomagnetic data in digital form compatible with computer processing with the least possible delay and would satisfy the recent request from related fields of geophysics. The new system was completed in August of 1972.

1.2 Design of a new system for standard magnetic observation at Kakioka

Recent development of electronics is changing the system of magnetic observation. Electronic devices using atomic or nuclear constant are replacing the classical instruments such as variometers of suspended bar magnet or magnetic theodolites. These new electronic magnetometers produce frequency outputs which are proportional to the field intensity, making automatic data processing possible. The absolute accuracy of the values measured by electronic magnetometers is high when instruments are designed carefully.

The possible finest time resolution at present is given by optical pumping magnetometer which indicates the Larmor frequency of alkali metal vapour under a magnetic field employing the technique of optical pumping (Bloom, 1962). The frequency is proportional to the field intensity at the absorption cell containing the vapour, with a possible shift in absolute value due to the cell parameters or circuit characteristics. Considering the recent request for magnetic observation, the optical pumping magnetometer is best for the primary sensor to detect the geomagnetic field, provided that the absolute value determination is carried out in other ways. The ASMO system proposed by Alldredge (1960) has been employed at some observatories using optical pumping magnetometers. It determines field values in a discrete time sequence, because each component is measured alternately by an optical pumping magnetometer sensor with bias coils. Future progress in geomagnetism or related fields may need a finer time resolution which can be attained by the optical pumping magnetometer.

In the new system of Kakioka, four optical pumping magnetometers are provided for four components of geomagnetic field, *i.e.* total force F , horizontal component H , vertical component Z and a special component H_y in the horizontal plane (Section 2.1). Each optical pumping magnetometer is equipped with a set of Helmholtz coils. According to the bias field of the Helmholtz coil, each sensor of the magnetometer produces a separate continuous frequency output which is proportional to a component. A time resolution of 0.01 second or better is easily obtained on a high speed analog record with a high sensitivity.

Digital sampling of the frequency in routine operation is at 3-sec intervals, or

every second upon request. Digital data is further processed in a data acquisition system designed for the new system, and an analog recorder monitors the operation with the normal speed of 20 mm/hour.

The absolute accuracy of the values obtained by optical pumping magnetometers is unfortunately not as good as that of the best instrument at present, though the shift in absolute value is fairly constant for a short time; hence calibration is necessary. The interval of the calibration depends on the stability of optical pumping magnetometers, for which 0.1γ /week or better is aimed at in the new system.

Proton magnetometers are considered now to be the best instrument for the absolute determination of the field intensity, though some problems remain (see Appendix). In order to determine all components of the field by the proton magnetometer, a rather complicated device is necessary. The geomagnetic field is divided into components, in general, according to the terrestrial coordinate which needs determination of true north and horizontal plane. This requires two turning axes of the instrument as well as a telescope for azimuth determination like a theodolite. Such a magnetometer theodolite of a proton sensor with orthogonal Helmholtz coil pairs must be complicated when an absolute accuracy of 0.1γ is aimed at for each component. In general a vector proton magnetometer determines the absolute value only for H and Z .

In the new system, a proton magnetometer is employed for the calibration of the total force and DI-72, a newly designed instrument (Section 2.7), measures D and I . The Helmholtz coil of the DI-72 nearly eliminates the total force of the geomagnetic field at its center. The residual transverse field is detected by a search coil situated at the center. When the field of the Helmholtz coil coincides with the reverse direction of the geomagnetic field, the induced AC voltage in the rotating search coil becomes zero. Thus the direction of the field can be read on the graduated circles attached to the Helmholtz coil. A telescope is provided at one end of the horizontal axis to determine the azimuth. The reason why the direction of the search coil is not read directly in a free field will be described in the study of the accuracy of the universal magnetometer A-56 in the Appendix. Details of the DI-72 is given in Section 2.7.

The vector proton magnetometer MO-P, which has been operated to obtain H and Z values at Kakioka since 1963, will supplement the calibration in the new system.

Output signals of the optical pumping magnetometers and the proton magnetometer are sent on line to computers of the data acquisition system in the new

system. Manual loading of the data is employed for the DI-72. The computer system processes automatically all data according to suitable programs. Processed data is stored in the magnetic disc memory, and can be retrieved in any of the output forms: digital magnetic tape, paper tape and printed table.

External digital data in magnetic tape, paper tape or card can also be read by the system. A curve follower and a curve plotter are provided for the input or output of analog records. Kakioka Magnetic Observatory operates two branch observatories: one at the northernmost of Japan, Memambetsu and the other at the southernmost, Kanoya (Fig. 1), where classical systems are still working. From analog magnetograms obtained at these observatories, digital values will be obtained semi-automatically by the curve follower connected to the computer system.

Details of the system instruments will be given in Chapter 2, and the operation and test results in Chapter 4.

A sizable area free from unwanted noises is necessary for installing the whole instruments of the system. Though artificial magnetic fields had generally been very small in the observatory ground, unnecessary old buildings were removed and a public road that ran through the planned site was eliminated to deny cars access to the ground. Also, undulation in the ground of the planned site was mostly eliminated. These modifications of the planned site were completed one year prior to the installation of our new system in order to allow the disturbed natural magnetic field of the site to settle.

A group of new houses built on the ground for magnetometer sensors are separated by at least 120 m from the control house which contains the main electronics and the data acquisition system. Highly non-magnetic materials only are used for the sensor houses which are separated from each other to avoid the influence of the bias field of the component magnetometer or the polarization field of the proton magnetometer.

These houses and the ground are described in Chapter 3.

Chapter 2. Instruments of the KASMMER System

2.1 Outline

The new system, which is constructed for standard magnetic observation at Kakioka according to the design described in the introduction, is called Kakioka Automatic Standard Magnetometer, KASMMER. The system mainly consists of

the following three parts:

1. Four optical pumping magnetometers by which total force F , horizontal component H , vertical component Z and a special component H_y of the geomagnetic field are measured continuously.
2. Calibration system which is composed of a proton magnetometer, the DI-72 and two large coil systems.
3. Data acquisition system which is composed of two mini-computers and accessories.

The outline of the KASMMER system is shown in Fig. 2. The D sensor of the optical pumping magnetometer produces signal frequencies in proportion to H_y (Fig. 3), not D . The reduction from H_y to D will be described later.

Continuous operation of four optical pumping magnetometers can give a comparison between the direct F value and the indirect one calculated from the H and Z values through the data acquisition system as well as each component value, so that the condition of the magnetometers also may be monitored continuously.

The sensor of a magnetometer is laid at the center of two orthogonal Helmholtz

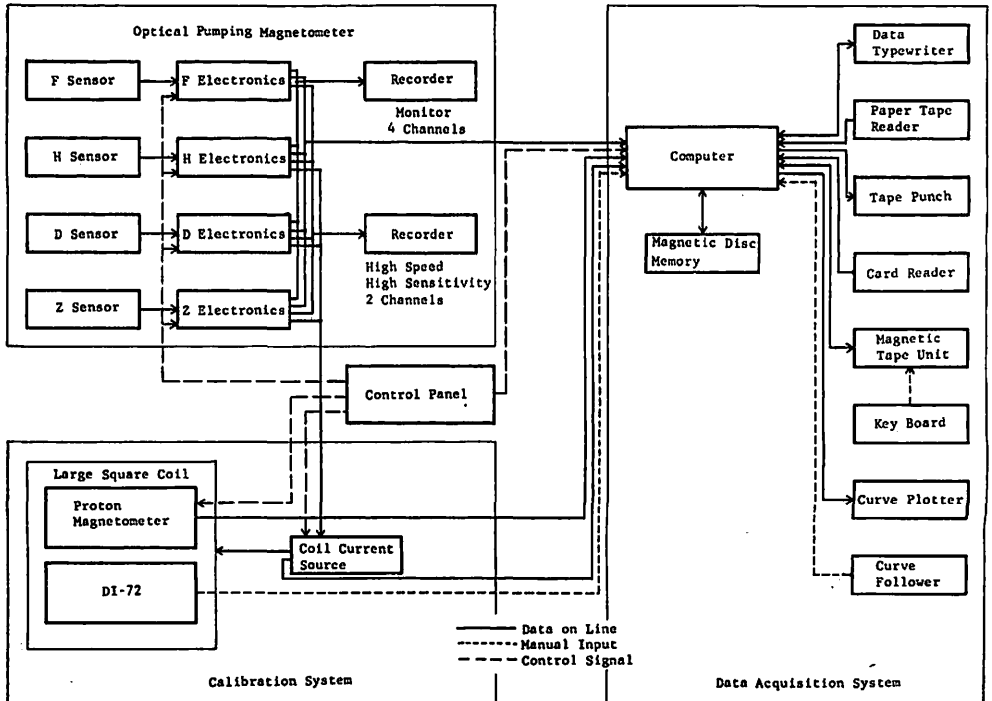


Fig. 2. Outline of the KASMMER system.

coil pairs. The component H or Z is measured by eliminating the perpendicular component in the same way as the vector proton magnetometer is operated. The two coil pairs facilitate many kinds of tests or exchange of the sensor assembly, though only one coil pair is necessary for the measurement of one component.

There are generally some problems on the measurement of D , because very small magnetic fields are not adequate for the usual optical pumping magnetometer. If the horizontal and the vertical components are eliminated from the geomagnetic field and a constant field of a suitable amount is added perpendicularly to the mean magnetic meridian, the change of D can be measured around the added field by the optical pumping magnetometer. However, it is not so easy to limit the change of the added field within 0.1γ or less for a long time. In the D optical pumping magnetometer of KASMMER, its sensor detects a force component H_y in the horizontal plane. The direction of the H_y makes an angle of 60° eastwards from the mean magnetic meridian (Fig. 3). The perpendicular components, H_x in the horizontal plane and Z , are eliminated by using the two orthogonal Helmholtz coil pairs.

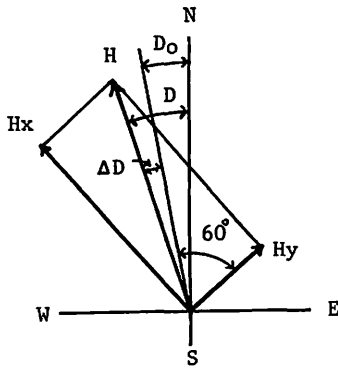


Fig. 3. Direction of H_y which is detected by the D optical pumping magnetometer.

The sensor of the F optical pumping magnetometer is laid also at the center of the similar Helmholtz coil pairs. Usually no bias field is applied, however the set can act as an ASMO system proposed by Alldredge for the measurement of the components when the proper instruments meet trouble.

Outputs of the optical pumping magnetometers are sent to the data acquisition system on line as well as to the analog recorders.

These magnetometers are calibrated by the proton magnetometer and the DI-72. Individual measured values of the calibration instruments may fluctuate more widely than those of the optical pumping magnetometer, though the former's mean gives more exact absolute value than the latter which includes a constant deviation to be determined by the calibration. In order to reduce the error of the individual fluctuation, the mean of many calibration measurements has to be used. On the other hand the natural magnetic field varies during a series of the measurements. Two ways are taken into consideration for the elimination of the time variation.

One is simply to compare the simultaneous values obtained by the calibration instruments and the optical pumping magnetometers. The computer system calcu-

lates the differences and gives their mean values and the error estimation. Another way is to eliminate the varying magnetic field by a suitable device at the location of the calibration instrument. A large coil system is provided for this purpose. It produces such a magnetic field as the time variation of the geomagnetic field is cancelled always in its central zone. It is so large that a few observers can operate the calibration instruments in it. The coil currents are regulated by the outputs of the optical pumping magnetometer.

The data acquisition system is a computer system including many accessories. The routine primary data processing gives the seven components, F , H , Z , D , I , X and Y at every minute. Hourly mean values are calculated from the 60 minute-values. Digital values of the seven components at any instant are also available. Further processing is made by putting suitable programs.

Using many kinds of the input and output devices and the attached external memory, various analyses of the data including external ones can be carried out for scientific use.

2.2 Optical pumping magnetometer

The optical pumping magnetometer of the KASMMER system employs a cesium oscillator as the sensing element to produce an output signal whose frequency is proportional to the magnetic field intensity at the sensor. The cesium sensor is laid at the center of Helmholtz coil pairs which produce a suitable bias field to measure a component. The assembly of the sensor and the coils is mounted on a granite pillar in a sensor house described in Section 3.3. Fig. 4 shows the assemblies for H and F . Four sensor houses each containing an assembly for F , H , D or Z measurement are well separated from each other. The output signals of the four sensors are sent to the electronics (Fig. 5) located in another house through coaxial cables in a duct. Fig. 6 shows major units of the four optical pumping magnetometers and their connection.

Temperature change of the sensor is kept to a minimum to avoid change in instrument parameter which may cause a shift in the absolute value of magnetic field. A half of the sensing element is contained in a thermos (Fig. 7), and its temperature is maintained at 40°C by using a heater and thermistors. Operating temperature being 60°C , the temperature of the lamp house is controlled separately. Major parts of the sensor electronics are also contained in thermostat boxes. Thus the temperature shift in oscillator frequency is mostly eliminated.

The thick line of the blockdiagram shows the main route of the signal. The frequency of the amplified signal is multiplied by 4. The electronic counter counts

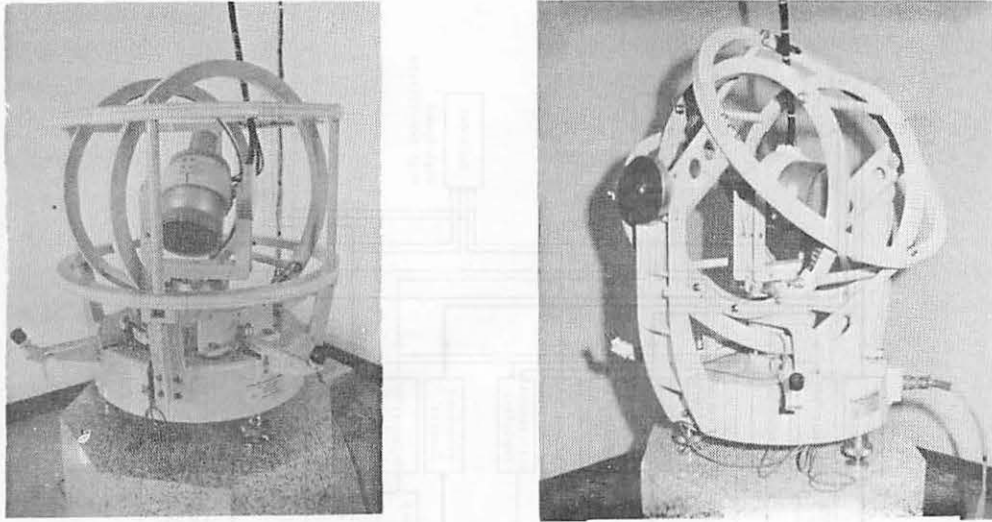


Fig. 4. Sensor of the optical pumping magnetometer with two orthogonal Helmholtz coil pairs for H (left) and F (right).

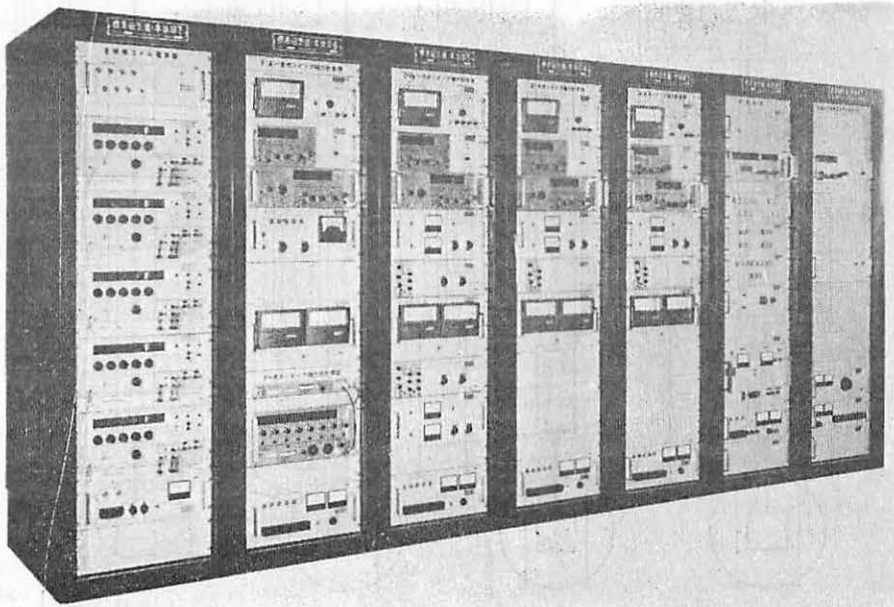


Fig. 5. Electronics of the optical pumping magnetometers and the proton magnetometer and the control panel.

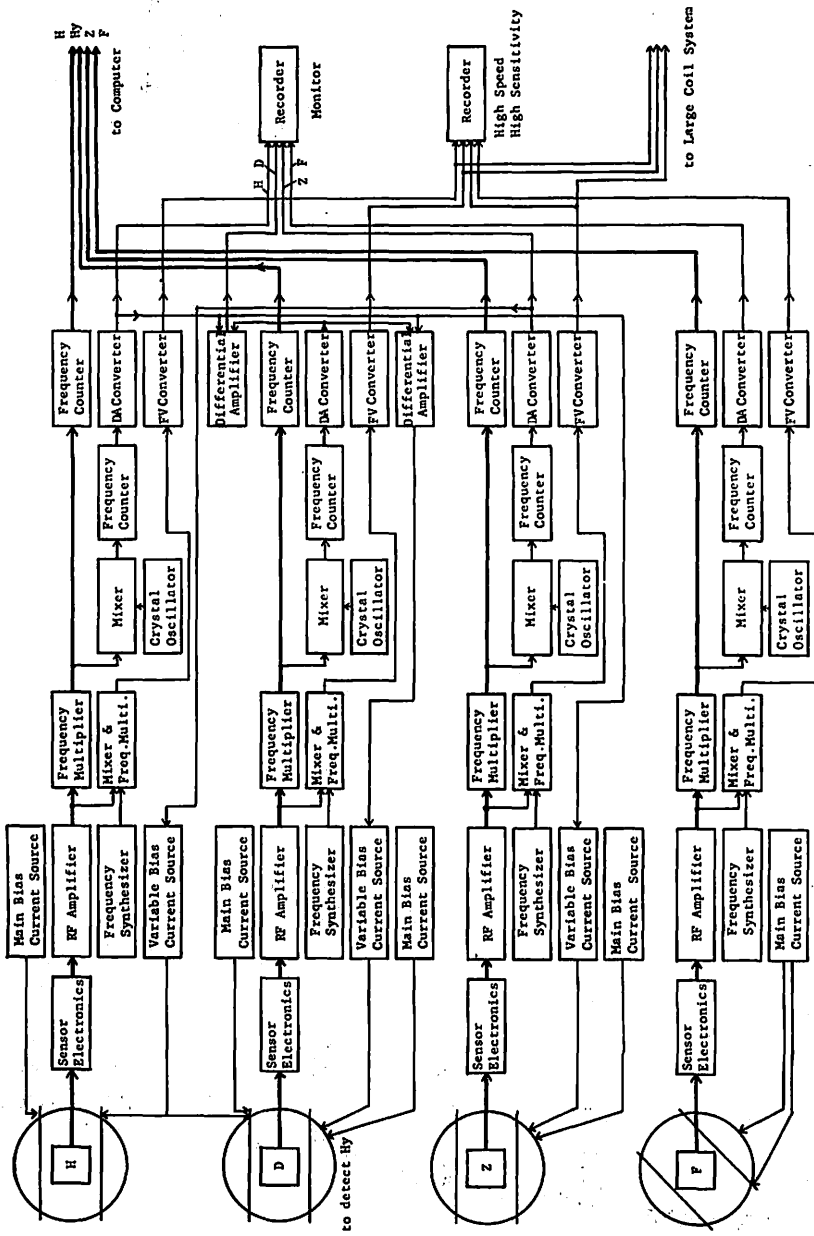


Fig. 6. Blockdiagram of the optical pumping magnetometers.

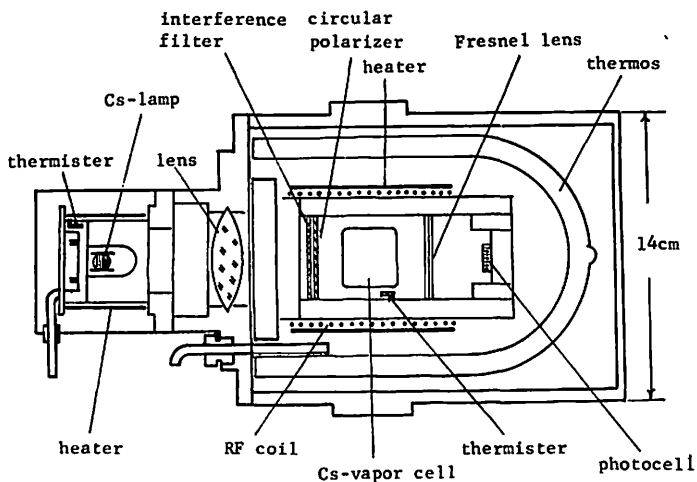


Fig. 7. Sensing element of the optical pumping magnetometer.

the multiplied frequency upon command for 1/1.4-sec gate, which is to give directly the γ value of the measured magnetic field in 0.1γ unit. The employed conversion constant, 1.4 MHz/gauss, comes from the Larmor frequency of C_{133}^{33} , 350 kHz/gauss, in a weak magnetic field. In the actual field, the Larmor frequency splits for different states of the angular momentum, therefore the output frequency of the cesium oscillator may deviate from 1.4 MHz/gauss depending on the characteristics of the individual instrument. However the deviation will be approximately constant, provided that the condition of the instrument is unchanged and that the magnetic field to be measured is not so deviated from the mean value.

The gate command is given from an electronic digital clock of the control panel at 3-sec intervals in the routine operation. If a finer time resolution of digital data is desired, the interval can be shortened down to 1 sec. The digital clock displays days-of-year, hours, minutes and seconds, and generates their BCD form outputs as well as time signals at intervals of 1 sec, 3 sec, 6 sec, 15 sec, 1 min, 10 min, 30 min, 1 hr, 12 hr and 24 hr for automatic operation of the KASMMER system. Its crystal oscillator is a very good frequency standard with a stability of 5×10^{-10} /day for the room temperature from 0 to 50°C.

Outputs of the counter are sent to the computer in BCD form together with those of the clock.

The multiplied frequencies are branched to a beat-down unit which consists of a mixer and a crystal oscillator. Its output frequencies are counted repeatedly by another counter, whose repeated counts are converted into a continuous analog

voltage through a DA converter. It is recorded on a 4-channel analog recorder with a speed of 2 cm/hour and with a full scale of 500γ . This is used as a monitor.

Another branch extends from the RF amplifier to produce an analog voltage with finer resolutions in both time and field value. The increment or decrement of the signal frequency from a given constant value is converted into proportional analog voltage by means of a frequency synthesizer and its accessories. The proportional voltage drives a current adjuster of the large coil system in the calibration system, and is recorded on a high speed analog recorder with high sensitivity upon request. Twelve speeds are available between 640 mm/min and 20 mm/hour. Small variations of 0.03γ can be detected over noise as are shown in Chapter 4.

The four optical pumping magnetometers are identical in construction. Because of different working ranges of the magnetic field for different components to be measured, the following channels are provided.

F optical pumping magnetometer

$46,000 \pm 1,000\gamma$	<i>F</i> channel
$48,500 \pm 1,000\gamma$	ASMO channel
$55,000 \pm 1,000\gamma$	AD channel for adjustment

H optical pumping magnetometer

$46,000 \pm 1,000\gamma$	<i>F</i> channel
$30,000 \pm 1,000\gamma$	<i>H</i> channel
$55,000 \pm 1,000\gamma$	AD channel for adjustment

D optical pumping magnetometer

$46,000 \pm 1,000\gamma$	<i>F</i> channel
$15,000 \pm 1,000\gamma$	<i>H_y</i> channel
$55,000 \pm 1,000\gamma$	AD channel for adjustment

Z optical pumping magnetometer

$46,000 \pm 1,000\gamma$	<i>F</i> channel
$34,500 \pm 1,000\gamma$	<i>Z</i> channel
$55,000 \pm 1,000\gamma$	AD channel for adjustment

The limitation of the range for each channel allows the use of band-pass filters in the sensor electronics, which increases the signal-to-noise ratio very much.

Each Helmholtz coil pair has to be oriented in a proper direction and its coil current has to be regulated to give a proper bias field for a specified component of the geomagnetic field to be measured. The procedure of adjusting the coil orientation and the current is roughly described for the *Z* optical pumping magnetometer in the following.

Two orthogonal Helmholtz coil pairs are mounted on a bed which can be turned on the vertical axis as described in Section 2.3. The axis of one Helmholtz coil pair approximately coincides with the vertical turning axis by design, and the other is approximately in a horizontal plane. Adjusting the level of the Helmholtz coil pairs, the vertical turning axis is made vertical at first. The horizontal axis of the Helmholtz coil is roughly aligned with the magnetic east-west direction. Applying a suitable amount of current for the coil positively and then negatively, the intensity of the vector sum magnetic field is measured through the AD channel of the optical pumping magnetometer. If there is a difference between the two values for positive and negative currents, the coil azimuth is re-adjusted until the difference disappears. Then, the Helmholtz coil pairs are turned 90° on the vertical axis to place the horizontal axis of the Helmholtz coil in the true magnetic north-south direction. If southward horizontal component added by thus oriented coil is exactly twice the horizontal component of the geomagnetic field, the intensity of the resultant magnetic field should be the same as the total intensity of the geomagnetic field. Therefore, by adjusting the coil current, the difference in magnitude between the total intensity of the resultant field and the geomagnetic field is reduced to zero. Then, the current is halved. By this procedure, the horizontal component of the geomagnetic field is nulled and the preparation for Z measurement is completed. Preparations for the other components are carried out similarly. If the horizontal axis of the Helmholtz coil is not exactly on the true horizontal plane due to mechanical construction, an error will occur in the Z values by the vertical component of the bias field created by the Helmholtz coil. Similarly in the other components, the parallel component of the bias field, which is produced by a small deviation of the Helmholtz coil axis from the plane normal to the component to be measured, will cause a direct error. These can be corrected by averaging two values measured at 180° -turned positions about the vertical axis in the same way as the vector proton magnetometer. However, in the continuous operation of the optical pumping magnetometer, the deviation of the measured values is corrected using a constant determined by calibration. Therefore, careful considerations are taken for stability of the fixed coil direction and of the pillar level not to change their initial values at least from one calibration measurement to the next.

A deviation of the Helmholtz coil field from the proper direction in the plane perpendicular to the component to be measured influences measurement much less than the said parallel component does, and can be neglected for practical purposes. Maladjustment of the coil current may also cause a very small error. Those of 77γ , 54γ and 83γ will cause only for an error of 0.1γ in H , H_y or Z value respec-

tively. More precise adjustment of the coil current can be achieved for a given instant, however, the time variation of the geomagnetic field will cause the composite field values exceed the limits (77, 54, 83 γ) afterwards. In order to cancel the time variation, an auxiliary winding is provided for each of the Helmholtz coils (Section 2.3).

2.3 Helmholtz coil pairs of the optical pumping magnetometer

The sensing element of the optical pumping magnetometer is laid at the center of two orthogonal Helmholtz coil pairs. The diameters of the coils are 50 cm and 60 cm. The coil pairs are fixed on a bed which can be turned on the vertical axis with a taper shaft bearing. The azimuth of the coil can be read to 0.1' from a graduated circle. A level of 10''-division is also provided. Stability tests have shown that the fluctuation of the vertical axis is less than a few seconds of arc for a full turn. This allows an operation, like in absolute measurement by a vector proton magnetometer, changing the azimuth of the Helmholtz coil. However a fixed position is employed for the routine operation to obtain continuous data, except the initial adjustment and occasional checking.

Each Helmholtz coil has two separate windings, main and auxiliary. The main winding supplies a constant field determined at the initial adjustment, whereas the auxiliary one cancels the time variation of the natural field. Various factors of the coils are shown in Table 1. A stabilized current source of 110 mA in full range is

Table 1. Factors of the Helmholtz coil.

	Winding	Approximate coil diameter mm	Turn	Coil constant γ /mA	DC resistance ohm
Helmholtz coil I	Main	500	360	1079	76.6
	Auxiliary	505	44	130	19.4
Helmholtz coil II	Main	600	280	1007	119.4
	Auxiliary	605	44	157	23.3

provided for the main winding. Its four step dials (the last one being at 10 μ A intervals) and a variable dial of 11 μ A in full range facilitate to adjust quickly the bias current. When the adjustment is completed, all dials are locked. The fluctuation of the current is less than 4×10^{-5} for ambient temperature of 15–30°C. Current is supplied to the auxiliary winding by a variable current source which is regulated by the output of the optical pumping magnetometer, so that it creates

the same magnetic field as the varying part of the corresponding component of the geomagnetic field.

The size and construction of the orthogonal Helmholtz coil pairs are the same for all magnetometers, whereas their orientations are different from each other as shown in Table 2.

Table 2. Orientations of the Helmholtz coil.

Magnetometer Helmholtz coil		F (for ASMO)	H	D	Z
I (500 mm)	Inclination	0°	—	0°	0°
	Azimuth	90°	—	-30°	0°
II (600 mm)	Inclination	41°	90°	90°	—
	Azimuth	0°	—	—	—

The angle shows the direction of the Helmholtz coil axis, which is perpendicular to the coil plane passing through the center, referred to the horizontal plane (for the inclination) and the magnetic meridian (for the azimuth).

The sensing element of the cesium oscillator is mounted on a holder which in turn is mounted on the bed of the Helmholtz coils (see the photograph in Fig. 4). The holder can be turned on a vertical axis which nearly coincides with the vertical axis of the coil bed. The sensing element also can be turned on a horizontal axis which passes through the center of the Helmholtz coil pairs. Thus the cesium light beam can be turned towards any direction, keeping the absorption cell at the center. Usually, 45° is employed for the angle between the light beam and the magnetic field to be measured. The direction is read to 0.1° from the graduated circles.

2.4 D measurement

The D optical pumping magnetometer gives originally the value of the H_y component (Fig. 3). Westward declination D is given by

$$D = D_0 + \Delta D = \cos^{-1} (H_y/H) + D_0 - 60^\circ$$

where D_0 and ΔD represent the mean and the increment of the westward declination respectively.

The computer system of KASMMER calculates the digital value of D from those of H_y and H according to the said equation, provided that D_0 is given as a constant determined by calibration measurements. On the other hand, analog values are composed in a differential amplifier by

$$\Delta D = C (\Delta H/2 - \Delta H_y)$$

where ΔH and ΔH_y are the increments of the corresponding components H and H_y , respectively, and C is a constant. The analog values of ΔH and ΔH_y are given by the DA converters of the H and D optical pumping magnetometers.

The orientation of the Helmholtz coil is shown in Table 2. With Helmholtz coil I eliminating the H_x component and coil II the Z component, the sensor detects the H_y component. After the initial adjustment of the coil current, time variations of the natural field are cancelled by the magnetic field produced by the auxiliary windings of the coil. The Z component of the auxiliary bias field is controlled by the output of the Z optical pumping magnetometer. In order to cancel the time variation of H_x component, it is necessary to know the variation itself. The increment ΔH_x of the H_x component is composed from ΔH and ΔH_y by another differential amplifier by

$$\Delta H_x = (1/\sqrt{3}) (2\Delta H - \Delta H_y)$$

The output of the differential amplifier regulates the variable current source for the auxiliary winding of Helmholtz coil I, so that the time variation of the H_x component is cancelled out.

A detailed study on the D measurement by an optical pumping magnetometer has been reported by Sano (1971).

2.5 ASMO system

The F optical pumping magnetometer usually gives the value of the total force only. However the attached Helmholtz coil pairs facilitate to operate it in the ASMO method proposed by Alldredge (1960). Component values obtained by this method could be substituted for the continuous values of the H , D and Z optical pumping magnetometers should they meet trouble.

The coil orientation is given in Table 2. Helmholtz coil I creates a constant

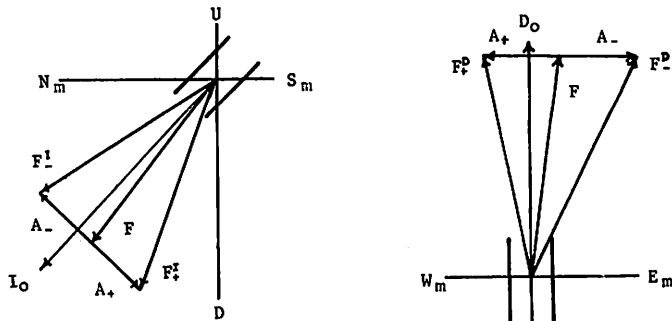


Fig. 8. Biased field in the ASMO method.

magnetic field A_+ westwards first, and then A_- eastwards (Fig. 8). The intensity of the vector sum of the magnetic field, F_{+^D} or F_{-^D} is measured by the magnetometer as well as F under no bias current. According to Allredge, westward declination D is given by

$$D = D_0 + \frac{(F_{+^D})^2 - (F_{-^D})^2}{2\sqrt{2} F \sqrt{(F_{+^D})^2 + (F_{-^D})^2} - 2F^2 \cos I_0}$$

where D_0 and I_0 are the mean declination and the mean inclination, respectively. Similarly inclination I is given by

$$I = I_0 + \frac{(F_{+^I})^2 - (F_{-^I})^2}{2\sqrt{2} F \sqrt{(F_{+^I})^2 + (F_{-^I})^2} - 2F^2}$$

using Helmholtz coil II.

These components are determined in sequential measurements for F , F_{+^D} , F_{-^D} , F_{+^I} , F_{-^I} and F , in this order. The computer system handles necessary computations.

2.6 Proton magnetometer

The proton magnetometer is a part of the calibration system (Fig. 9) of KASMMER, and determines the absolute value of the total force. Its sensing

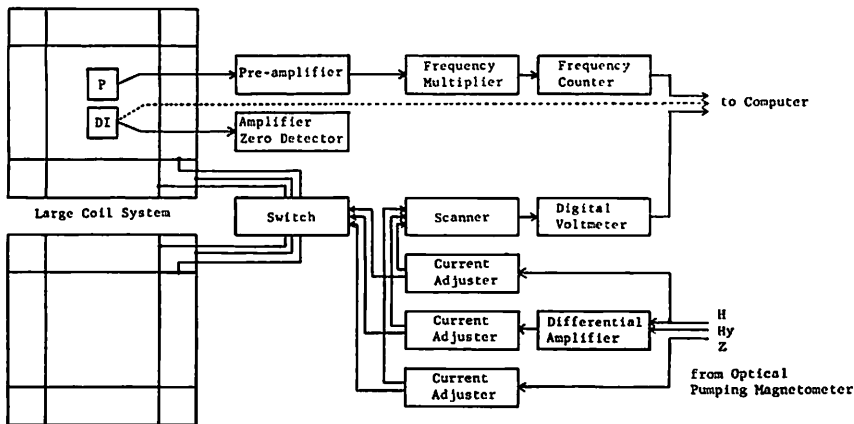


Fig. 9. Outline of the calibration system.

element is hung from the ceiling of calibration house 1 (Section 3.4) above the DI-72 which forms another part of the calibration system (Section 2.7). Materials of the sensing element have been carefully tested by an astatic magnetometer or an optical pumping magnetometer to exclude even a slight trace of magnetic substances,

because the strong polarizing field may cause an asymmetrical distribution of the magnetization which may result in a change of the measured value of the total force (see Appendix). Generated signal is amplified by a preamplifier in the house, then conveyed over a coaxial cable to the electronic devices in the control house.

The signal frequency is multiplied by 200. An electronic counter counts the multiplied frequency, giving the digital value in 0.1γ unit for 1.17437 sec gate determined by the gyro-magnetic ratio,

$$\gamma_p = 2.67513 \times 10^4 \text{ sec}^{-1} \text{ gauss}^{-1}$$

The process of polarizing and counting of the generated signal frequency can be repeated automatically at 6-sec intervals besides a manual command. The output of the counter in BCD form is sent to the computer system on line together with the digital time.

Another sensing element is provided to survey the distribution of the total force in the calibration house and to watch its secular variation.

2.7 DI-72

The DI-72 is a magnetometer theodolite newly designed for KASMMER to measure declination D and inclination I , with a Helmholtz coil mounted on a theodolite and a rotating search coil at its center. The Helmholtz coil creates a magnetic field \vec{F}_c whose intensity F_c is approximately equal to total intensity F of the geomagnetic field \vec{F} . Changing the direction of \vec{F}_c to approach the just reverse of \vec{F} , the transverse component ΔF_s of the vector sum, $\vec{F}_c + \vec{F}$, is detected by the rotating search coil whose axis is lying along \vec{F}_c (Fig. 10). When the output AC signal of the search coil becomes zero, the direction of \vec{F}_c coincides with that of $-\vec{F}$. Using this null method, declination D and inclination I of the geomagnetic field \vec{F} are measured as the direction of the Helmholtz coil.

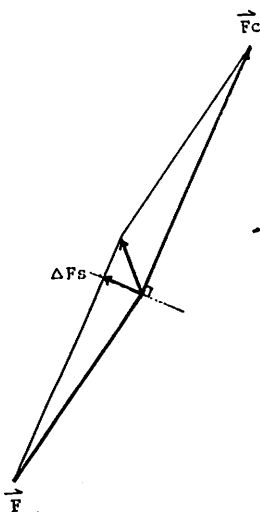


Fig. 10. Transverse fields ΔF_s which is detected by the search coil of the DI-72.

The given F_c may differ from F by a small quantity $\Delta F (= F_c - F)$, and the direction of the rotation axis of the search coil also may deflect from \vec{F}_c by a small angle $\Delta\theta$ with an azimuth φ from the plane including \vec{F}_c and \vec{F} (Fig. 11). Here, $\Delta\theta$ is a constant determined by the mechanical construction of the coils.

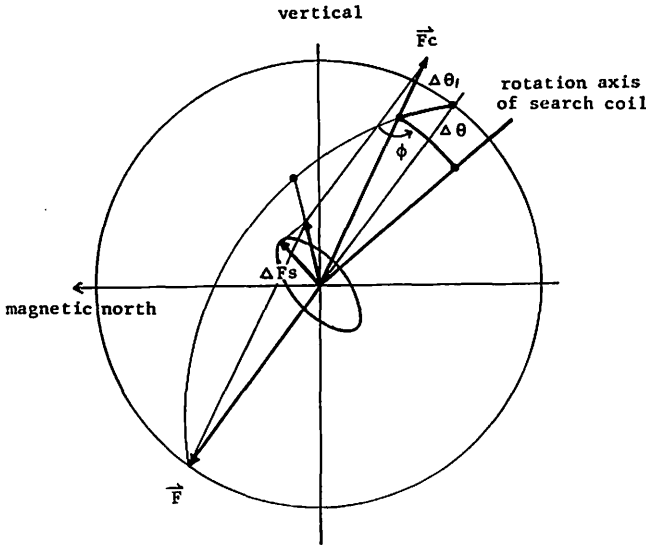


Fig. 11. Direction of the rotation axis of the search coil.

On the other hand, φ may change as the direction of \vec{F}_c is changed around that of $-\vec{F}$. When the angle between \vec{F}_c and \vec{F} is $\pi - \Delta\theta_1$, intensity of the magnetic field perpendicular to the rotation axis is given by

$$\Delta F_s = F \sqrt{(\Delta\theta_1)^2 - 2 \frac{\Delta F}{F} \Delta\theta_1 \Delta\theta \cos \varphi + \left(\frac{\Delta F}{F} \Delta\theta\right)^2}$$

with small quantity of higher order neglected. The rotation of the search coil produces an AC electromotive force whose amplitude is proportional to ΔF_s . Changing the direction of \vec{F}_c , ΔF_s is brought to zero at

$$\Delta\theta_1 = \frac{\Delta F}{F} \Delta\theta \quad \text{and} \quad \varphi = 0$$

The null method gives only a small error of second order, $(\Delta F/F) \Delta\theta$, in the direction determination of \vec{F} .

If $\Delta F = 100 \gamma$ and $\Delta\theta = 4'$, the error is less than $0.01'$ for $F = 46,000 \gamma$ which is approximately the total intensity of the geomagnetic field at Kakioka. The limits of 100γ and $4'$ are easy to attain by the adjustment of the coil current and coil construction. This method definitely reduces the error caused by the fluctuation of the rotation axis due to the clearance of the bearing, compared with the direct use of a rotating search coil to find the field direction.

The diameter of the Helmholtz coil is approximately 30 cm. The 200-turn winding of copper wire generates a uniform magnetic field of approximately $1200 \gamma/\text{mA}$ in the central zone. With the telescope moved to one end of the hori-

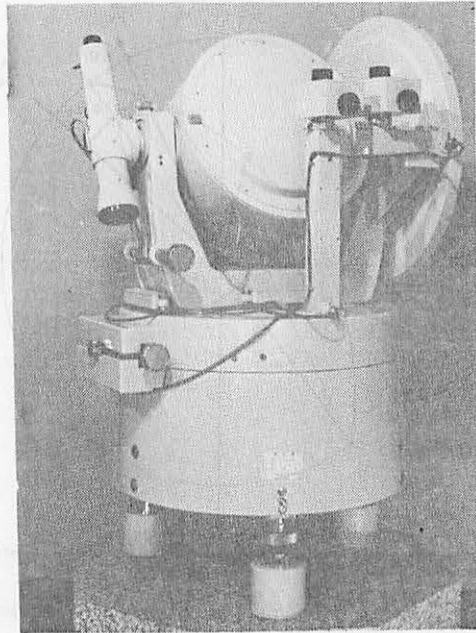


Fig. 12. The DI-72.

zontal shaft of the theodolite, the Helmholtz coil is mounted on the horizontal shaft like a telescope of a conventional theodolite (Fig. 12). The center of the Helmholtz coil pair coincides with the center of the theodolite, and the coil plane is parallel to the horizontal axis. \vec{F}_c is created in the direction of the Helmholtz coil axis which is normal to the coil plane passing through its center.

The dip and declination of the Helmholtz coil axis are read to $1''$ by means of microscopes with optical micrometers, from the vertical and the horizontal circles graduated to $10'$. The mean error of the graduation and the micrometer reading is estimated at $0.2''$ or less.

The search coil, a circular coil of 115,000-turn winding and maximum diameter 4.4 cm, is located at the center of the Helmholtz coil, supported by a frame which can be turned independently on the horizontal axis of the Helmholtz coil. The search coil can be rapidly rotated on an axis lying along a diameter of the coil. Though the rotation axis of the search coil and the F_c lines rotate independently, their turning axes are strictly the same, *i. e.*, the horizontal axis of the Helmholtz coil. The rotation axis of the search coil can be locked with respect to the Helmholtz coil at angles of 0° , 90° , 180° and 270° from the Helmholtz coil axis. Fig. 13 shows the 90° position.

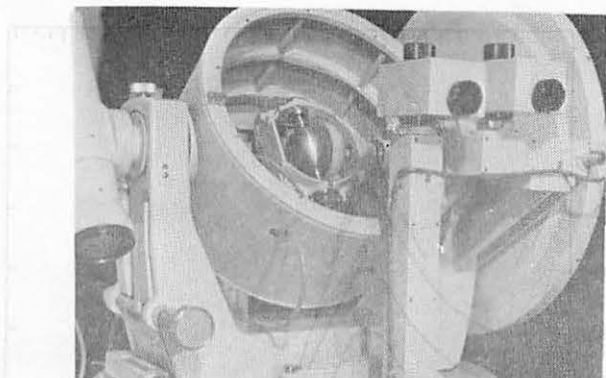


Fig. 13. The Helmholtz coil of the DI-72. Note the mechanisms within.

The search coil is manually driven with a shaft passing through the center of the horizontal axis and a bevel gear in the frame. The rotation of 10 cycles/sec generates an AC electromotive force of $1.9 \mu\text{V}$ under a magnetic field of 1γ . At the outside end of the shaft an on-off contact is provided to generate a synchronized signal for the trigger of the synchroscope in the signal detector.

All parts of the DI-72 are made of highly non-magnetic materials examined by an astatic magnetometer or an optical pumping magnetometer. Unwanted magnetic field is considered to be less than 0.1γ at the center.

The AC signals are amplified by a low-noise amplifier which employs operational amplifier units (Fig. 14). Twin-T filters in the negative feedback circuit

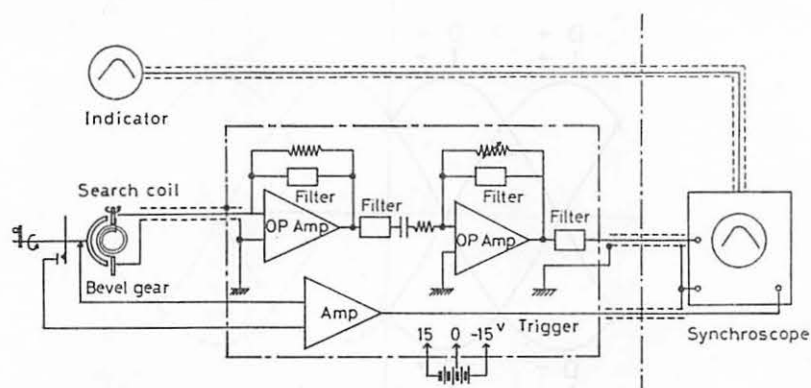


Fig. 14. Amplifier to detect the signal from the search coil on rotation.

reject noises of 50 Hz coming from commercial power line. The filters' band-pass character of around 10 Hz (Fig. 15) permits fluctuations in frequency of manual rotation, which is generally in a range from 8 to 12 Hz. When the search coil is

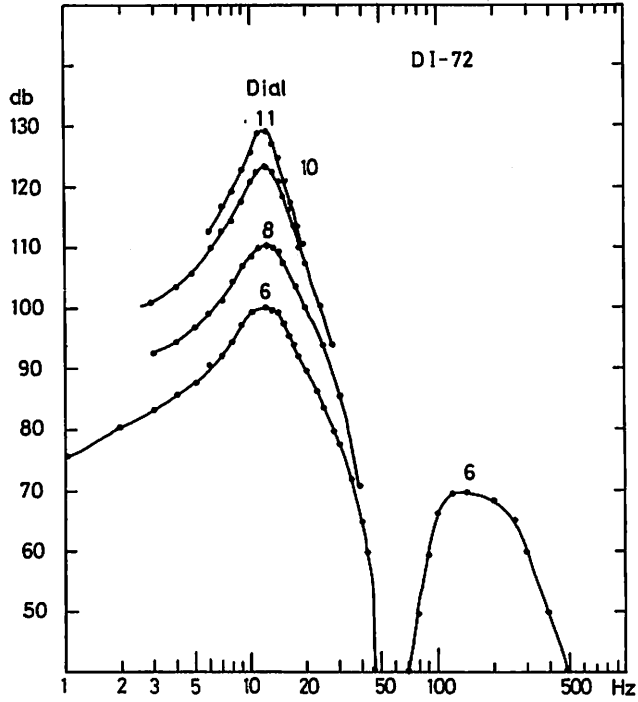


Fig. 15. Frequency response of the amplifier.

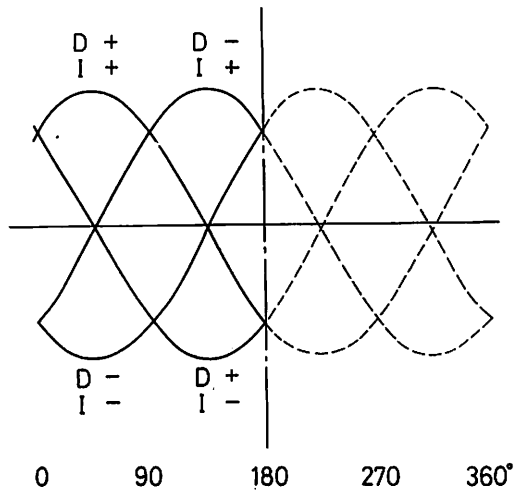


Fig. 16. Synchroscope figure of the search coil signal when F_C deflects from $-F^*$ by a small angle towards the indicated direction.

rotating, the noise from the connected amplifier is only once or twice in a minute with peak-to-peak amplitudes of less than $0.3 \mu\text{V}$ corresponding to 0.15γ . The noise occurrence being so infrequent, signals of 0.1γ or less are easily detected.

Output signals of the amplifier are displayed on a synchroscope. Watching the synchroscope figure, the observer adjusts the direction of the Helmholtz coil by means of two tangent screws of the theodolite, one for azimuth and the other for inclination. The direction of the detected field is known by the phase shift of the figure relative to the trigger pulse, and the intensity of the field by its amplitude (Fig. 16). The observer can immediately decide which screw should be turned to reduce the signal.

The cathode-ray tube of a synchroscope is detached and placed inside calibration house 1 for easy observation, whereas the rest of the synchroscope is placed outside with a shelter. The magnetic field caused by the synchroscope is thus reduced to a negligible amount, less than 0.1γ , at the place of the magnetometer theodolite.

At the beginning of a measurement, the rotation axis of the search coil is locked in a position parallel to the Helmholtz coil axis. With no current fed to the Helmholtz coil, the direction of the rotation axis is changed to coincide approximately with the geomagnetic field \vec{F} by detecting the AC signal of the search coil in a similar way as an earth-inductor. The rotation axis of the search coil being locked to the Helmholtz coil, the Helmholtz coil axis also comes approximately to the direction of \vec{F} . And then, the rotation axis is turned 90° or 270° so that it becomes perpendicular to the Helmholtz coil axis whose direction is held unchanged. Giving a current to the Helmholtz coil to create a magnetic field \vec{F}_c in the reverse direction of \vec{F} , the difference $\vec{F}_c - \vec{F}$ is detected by the rotation of the search coil in the perpendicular position. The current is varied until the difference becomes zero and the current is held at that value, and the rotation axis of the search coil is returned to the parallel position. Preliminary adjustment thus completed, the measurements of D and I are ready to be started.

Parallel and perpendicular positions of the rotation axis have mechanically been predetermined, and the axis can be brought to and locked at a desired position by a one-touch operation. Orientation error $\Delta\theta$ for each position is approximately $1.5'$ which is well below the $4'$ limit for the accuracy of $0.01'$ or 0.1γ . On the other hand the fluctuation of the rotation axis is $5''$ on rotation, which directly limits the accuracy of the direction determination when the search coil is used directly under no current of the Helmholtz coil. The accuracy of $5''$ itself is better than $0.1'$ of ordinary magnetometer theodolites such as GSI (Tsubokawa 1951 a, b), therefore, this preliminary adjustment suffices to measure D and I roughly. For the expected

high accuracy of the KASMMER system, the main procedure starts from this rough adjustment.

Watching the output signal of the search coil on rotation in the parallel position, fine adjustment of the Helmholtz coil direction is carried out until the signal reduces to zero. At the zero signal, the direction of the Helmholtz coil axis gives the exact direction of the geomagnetic field. The orientation error $\Delta\theta$ ($=1.5'$) of the search coil will not produce an error more than $0.01'$, as described above, provided that ΔF is less than 100γ . It is also clear that difference ΔF ($=F_c - F$) is far below 100γ at the initial adjustment, and that the time variation of F usually will not exceed 100γ during the period of one series of measurements.

The direction of \vec{F}_c , which coincides approximately with the mechanical axis of the Helmholtz coil, is in general deviated by a small angle from the plane normal to the horizontal axis which is also in general deviated by another small angle from the exact horizontal plane. The errors caused by these deviations are cancelled out by averaging two values measured at 180° -turned positions about the vertical axis in the same way as in ordinary theodolite operations, except a small quantity of higher order. Similarly, the error due to a small deflection of the vertical axis from the exact vertical line is corrected by readings of the attached levels graduated to $5''/2$ mm.

Each of the 180° -turned positions of the Helmholtz coil about the vertical axis is called here H_E (when marked side pointed to east) and H_W (west) respectively. In each position, measurements are carried out in two rotational senses, R for right-handed rotation and L for left-handed rotation of the search coil. A set of four measurements, *i. e.*, R and L for each of H_E and H_W , gives one value for each of D and I .

The Helmholtz coil can be turned on the horizontal axis. Measurements are repeated again turning the coil upside-down. The respective positions are H_U (marked side up) and H_D (down). The rotation axis of the search coil also can be turned independently on the same horizontal axis, and the measurements are carried out for both of the positions, S_U and S_D which are similarly defined. The angle between the Helmholtz coil axis and the rotation axis of the search coil is 0° for (H_U, S_U) and (H_D, S_D), and 180° for (H_U, S_D) and (H_D, S_U).

Total combinations of (H_E or H_W), (R or L), (H_U or H_D) and (S_U or S_D) make up sixteen elements, which form one set of measurements. If there is no systematic error between the up-down positions of the Helmholtz coil or the rotation axis of the search coil, a set of measurements will give 4 values for each of D and I .

The time variation of the geomagnetic field is corrected for each one of the

16 elements by using the values simultaneously obtained by the optical pumping magnetometer. Or measurements are carried out with the time variation automatically nulled by the large coil system described below. And the DI-72 is laid at the center of this large coil system.

2.8 Large coil system

The large coil system located in calibration house 1 is to create a large space of a constant magnetic field free from the time variation of the natural field. Three coil pairs, C_H , C_D and C_Z , are provided for the three components, H , D and Z , of the geomagnetic field. Each coil pair consists of two identical 3-m square coils placed in parallel and 1.632 m apart. A series current on the coil pair will produce a uniform magnetic field in a rather large space around the center. Three coil pairs form an orthogonal system fixed on a large supporting bed which has three adjustable legs. Each leg stands on a separate granite pillar (see Fig. 26 of Section 3.4). The azimuth and the level of the coil system are adjusted by the legs at the initial setting in such a way that the axes of the coil pairs approximately point magnetic north, magnetic west and downwards, respectively, for C_H , C_D and C_Z . The axis of a coil pair means the normal of the coil planes passing through the center of both coils.

For each coil pair, current is regulated automatically by the output of the optical pumping magnetometer so as to create the same magnetic field negatively as the increment of the corresponding component of the geomagnetic field from a given constant value.

The magnetic field in the central part of the coil system remains at a constant throughout the operation. The ratio of the current to the output voltage of the magnetometer is adjusted initially by the current adjuster (Fig. 9). The computer system checks the amount of current.

Strictly speaking, the variation in the geomagnetic field can not completely nulled due to a difference in orientation between this coil system and the optical pumping magnetometers. In order to reduce the residual field, a secondary winding of 4 turns is provided for each coil besides the main winding of 20 turns. A suitable distribution of coil currents will reduce the residual field to zero.

A tall granite pillar mounted on an underground foundation passes through a large hole in the coil bed (Fig. 26).

Two identical large coil systems are arranged symmetrically in calibration house 1, one to the east and the other to the west. The west system provides a constant field to calibrate other magnetometers. There is much merit of the coil system

for the calibration of classical type magnetometers which need much time to complete a single measurement.

2.9 Data acquisition system

All digital data obtained by KASMMER is processed in the data acquisition system which is a computer system with various accessories (Fig. 17). Two mini-computers, HITAC-10, are employed for the calculation. A magnetic disc memory of 650 kW supplements the core memory of 16 bits, 8 kW in each computer.

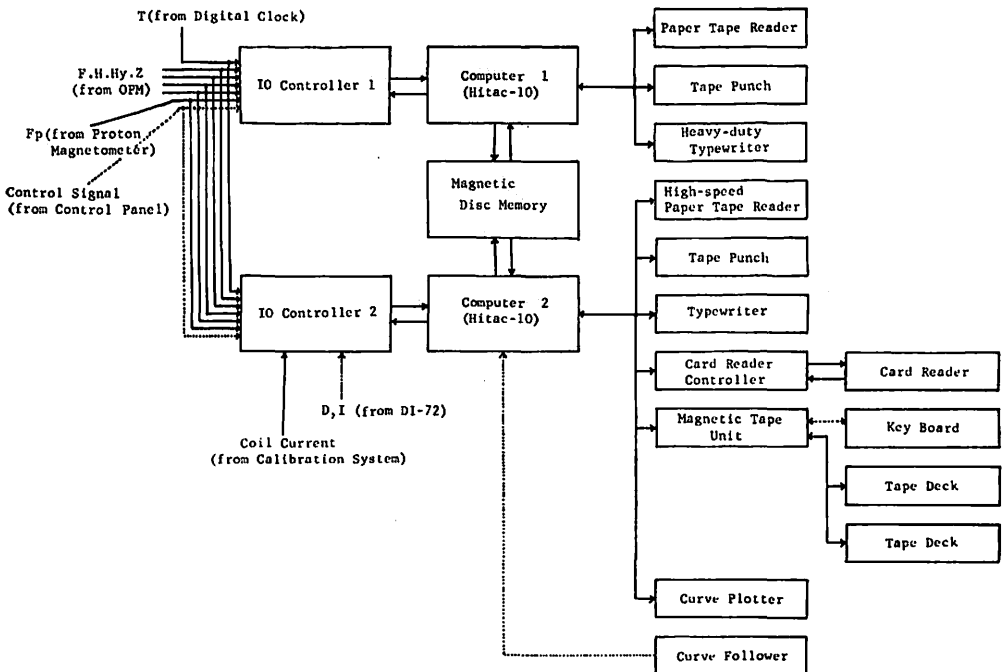


Fig. 17. Blockdiagram of the data acquisition system.

A paper tape reader, a tape punch and a heavy-duty typewriter are attached to computer 1 which calculates routine data. Processed data of the seven components of the geomagnetic field, F , H , Z , D , I , X and Y is initially stored in the disc memory and typed out periodically.

Computer 2 calculates calibration data, and is used also for nonperiodical processings. A high-speed paper tape reader, a tape punch, a data typewriter, a card reader, a digital magnetic tape unit, a curve plotter and a curve follower are attached to computer 2. The card reader reads 80-column cards at a speed of 400 cards/sec. The digital magnetic tape unit contains a key board as well as two

tape decks for recording and reading. Routine data is transferred to 9-track digital magnetic tape through computer 2 before the over-flow of the disc memory occurs. The tape width and the reel diameter are 1/2 and 8½ inches respectively. Direct manual data input to the magnetic tape is performed by the key board with facilities for typing, checking and correcting for any specified parts of the tape. Two tape decks make it easy to get a copy of the magnetic tape.

The curve plotter (*X-Y* plotter WX 535, Fig. 18) writes figures or analog records according to the input pulses given by computer 2. A suitable interface

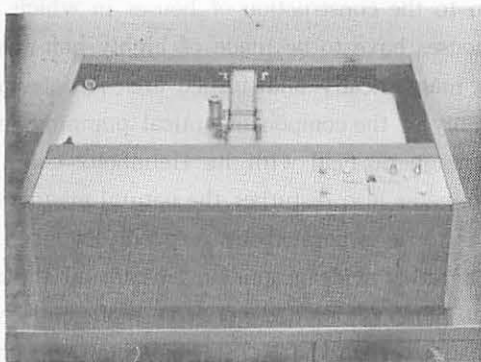


Fig. 18. Curve plotter.

is provided to connect with the computer as well as a subroutine assembler. On the other hand, the curve follower semi-automatically digitizes analog records. Coordinates of a curve are digitized automatically in 0.1 mm unit when the attached tracer follows the curve of the record paper mounted on the deck of the instrument (Fig. 19). The tracer is driven along abscissa by one of the three ways: manually, and automatically at constant speed or in steps changeable from 0.2 to 10 mm.

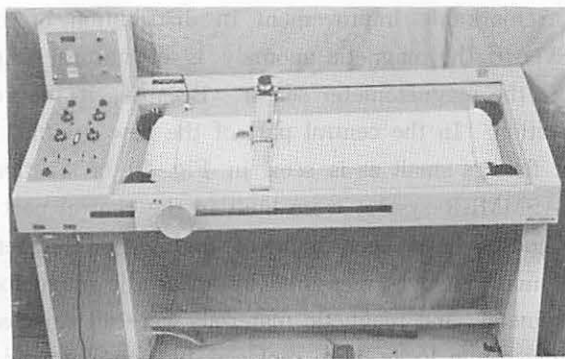


Fig. 19. Curve follower.

When the tracer is automatically driven along the abscissa, the tracer is to be manipulated along the ordinate only.

Chapter 3. Observation Houses

3.1 General layout of the ground and houses for the KASMMER

When planning geomagnetic observation of a high accuracy, careful consideration has to be given to the construction of houses in which magnetometer sensors are installed. The houses have to be made of highly non-magnetic materials, and have to be built in a magnetically undisturbed area free from artificial fields.

The sensor assembly of the component optical pumping magnetometer produces an external artificial magnetic field with its Helmholtz coil. The polarizing field of the proton magnetometer also disturbs the natural magnetic field in its surroundings. Each sensor has to be separated by a good distance to detect the natural field. This requires a rather wide ground to allocate all the sensors.

Kakioka Magnetic Observatory had not have sufficiently wide vacant area free from artificial disturbances when the KASMMER plan was conceived. A new site was prepared in the southern half of the observatory ground (Fig. 20). A few old houses in the area were removed and the lower eastern half of the site is filled with the earth from the higher western half.

The newly prepared ground, approximately 13,000 m², is flat, with a slight northward slope for drainage. The east side and south side are bounded by low-lying farm fields with a drop of 10 m at maximum. The other sides are joined naturally to the undulating land except a small drop near the southwest corner.

Magnetic surveys carried out before and after the construction of the new ground show a remarkable improvement in distribution of magnetic anomalies (Section 3.6). Even if the magnetic anomaly is of natural origin, it is better to avoid it to locate the magnetometer sensor. Because, it may cause an unwanted local secular variation. In the central part of the new ground, the gradient of the natural magnetic field is small as is seen in Fig. 29 of Section 3.6. New sensor houses of the KASMMER system were built in the central part (Fig. 20).

The sensor houses have been built of highly non-magnetic materials. The magnetism of all materials was measured by an astatic magnetometer or an optical pumping magnetometer, and magnetic materials were all rejected. Even steel pins or springs in hinges or in locks were replaced by non-magnetic metals. Thus the resultant distortion of the natural field is less than 0.1 γ .

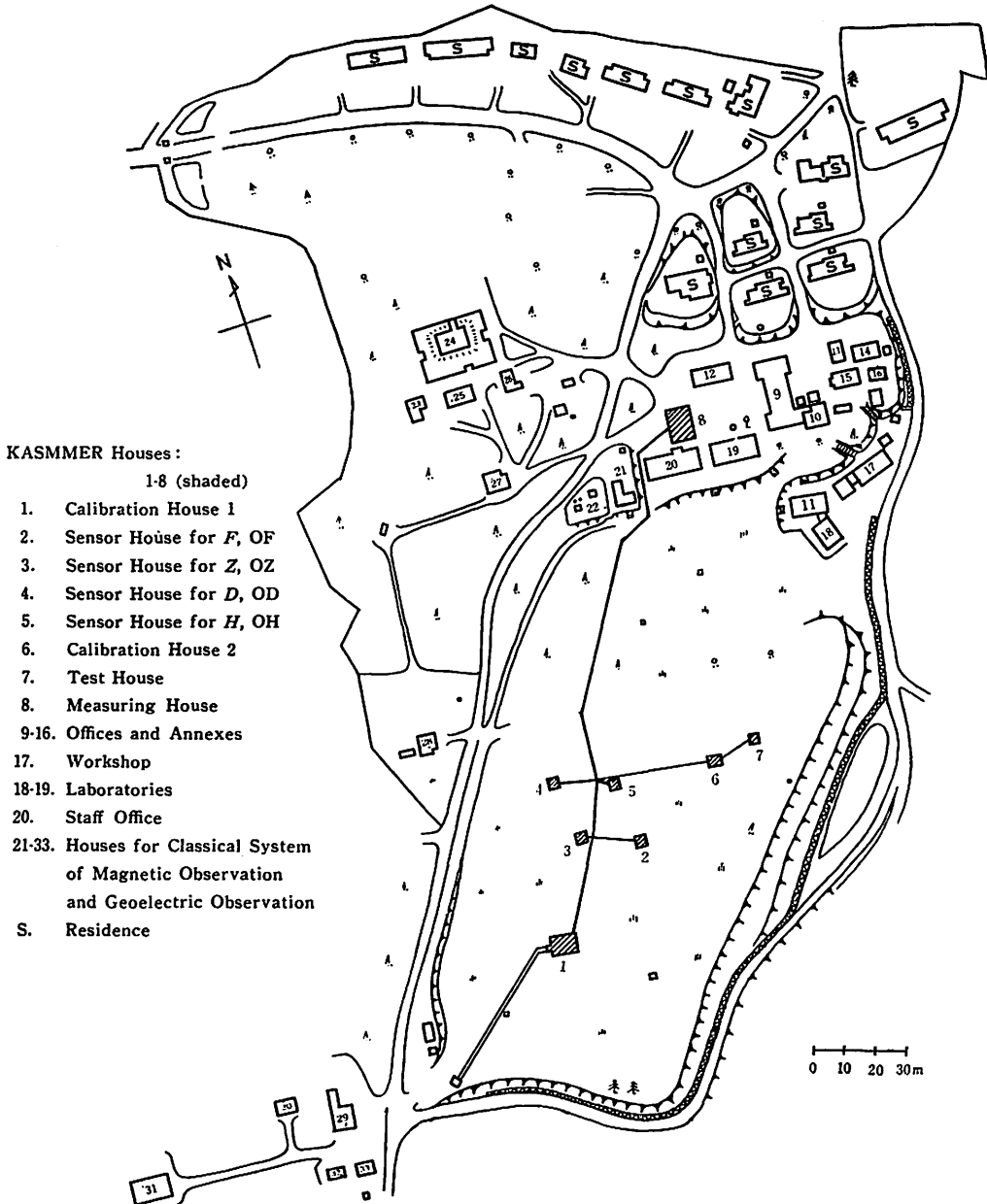


Fig. 20. Ground and houses of Kakioka Magnetic Observatory.

On the other hand, the construction of a pillar, on which the instrument is laid, inevitably causes a slight distortion in the natural field. Because, some soil has to

be removed to construct the foundation. The magnetic susceptibility of the soil in the site is, generally, $0.6\sim 1\times 10^{-3}$ emu/cm³. The pillar makes a magnetically hollow space in the uniform soil.

In order to get high stability of the pillar, its underground part has to be large. For the sensor of the component magnetometer, a change in pillar inclination directly causes a change in measured value (Section 2.2). A bigger foundation is better on this point. However it inevitably results in a considerable distortion of the natural field at the sensor. The field distortion might be constant for a long time, giving no trouble in the geomagnetic observation. Nevertheless it is clearly better to reduce such distortion.

If the underground part of the pillar is made of some material whose magnetic susceptibility is the same as that of the soil, the field will not be distorted at the initial time. But, the magnetism of the material might change afterwards, causing a local secular variation. This method is not employed in the KASMMER system, because the use of unnatural substances with magnetism bears much uncertainty.

With a taller pillar, the distortion of the field may be smaller at the sensor laid on the pillar. However, the stability requirement demands a larger foundation which makes the magnetically hollow space larger. For the component optical pumping magnetometer, the pillar's stability is regarded as of greater importance than the field distortion. Shorter fluctuations of the pillar inclination, such as diurnal variation, has to be avoided, because there are no means of correction in the routine operation. The change in the field distortion, if any, is considered to be slow, and it can be corrected by periodical calibration measurements.

For the pillar of the calibration instrument on the other hand, the reduction of the field distortion is more important. A slight change in the pillar inclination, if it occurs, can be adjusted by the instrumental level or corrected by level readings whereas a change in the field distortion cannot be separated from the natural secular variation in the geomagnetic field. Details of the pillar will be shown in the later sections.

Heat insulating materials are used for the sensor houses to reduce the rapid change in room temperature. The sensor house of the calibration instruments is air-conditioned because the DI-72 has to be operated within $20^{\circ}\pm 5^{\circ}\text{C}$ and preserved within $20^{\circ}\pm 10^{\circ}\text{C}$ to keep its precision.

All equipments having magnetism, such as main electronics, recorders and data acquisition system, are located in a building (control house) constructed near the staff office (Fig. 20). It is separated approximately 120 m from the nearest sensor house. The operation of the KASMMER system is controlled from this control house.

3.2 Arrangement of sensor houses

The locations of the sensor houses are decided considering the following points:

- 1) Along the south and east boundaries of the new ground, there is a small road through which small cars can run, though the car traffic is rare.
- 2) Local magnetic anomalies are rather intense along the boundary due to undulation and buildings outside the ground.
- 3) To assure better stability of the pillar, it is better to construct the sensor house on the ground where surface soil was merely removed, with the subsoil undisturbed.
- 4) The sensor of the proton magnetometer produces a magnetic field which extends over a rather wide area.
- 5) The Helmholtz coil of the component optical pumping magnetometer also generates a magnetic field around it.

Considering 1)–3), all sensor houses have to be built in the central zone of the ground. And, 4) and 5) require sufficient separation among sensor houses.

The polarizing field of the proton magnetometer is perpendicular to the magnetic meridian plane at the sensor. Its magnetic moment M_p produces a magnetic field:

$$\begin{aligned} \Delta H_p &= 3 (M_p/r^3) \sin \varphi \cos \varphi \\ \Delta H_{y_p} &= (M_p/r^3) \{ (\sqrt{3}/2) (3 \sin^2 \varphi - 1) + (3/2) \sin \varphi \cos \varphi \} \\ \Delta Z_p &= 0 \\ \Delta F_p &= 3 (M_p/r^3) \sin \varphi \cos \varphi \cos I \end{aligned}$$

at a distance r and an azimuth φ measured from the magnetic north in the same horizontal plane (Fig. 21), where ΔH_p , ΔH_{y_p} , ΔZ_p and ΔF_p are the components along H , H_y , Z and F , respectively, and I is the inclination of the geomagnetic field. Subscript p signifies the effect due to the proton magnetometer.

Similarly the vertical magnetic moment M_H of the Helmholtz coil of the H optical pumping magnetometer generates the effect,

$$\begin{aligned} \Delta H_H &= 0 \\ \Delta H_{y_H} &= 0 \\ \Delta Z_H &= M_H/r^3 \\ \Delta F_H &= (M_H/r^3) \sin I \end{aligned}$$

where the notations are the same as the previous ones for the proton magnetometer except subscript H which signifies the source magnetometer. Using

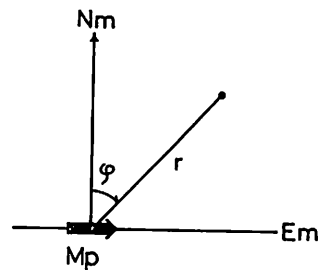


Fig. 21. Distance r from magnetic moment M_p and azimuth φ from the magnetic meridian plane.

similar notations again, the effect of the Z optical pumping magnetometer is given by

$$\begin{aligned} \Delta H_z &= - (M_z/r^3) (3 \cos^2 \varphi - 1) \\ \Delta H_{yz} &= - (M_z/r^3) \{ (1/2) (3 \cos^2 \varphi - 1) + (3\sqrt{3}/2) \sin \varphi \cos \varphi \} \\ \Delta Z_z &= 0 \\ \Delta F_z &= - (M_z/r^3) (3 \cos^2 \varphi - 1) \cos I \end{aligned}$$

The D optical pumping magnetometer utilizes two Helmholtz coils whose magnetic moments are M_{D1} for the vertical one and M_{D2} for the horizontal one. The magnetic field produced by the moments is given by

$$\begin{aligned} \Delta H_D &= (\sqrt{3}/2) (M_{D2}/r^3) \{ 3 \sin(\varphi - 60^\circ) \cos \varphi + (\sqrt{3}/2) \} \\ \Delta Z_D &= M_{D1}/r^3, \\ \Delta F_D &= (M_{D1}/r^3) \sin I + (\sqrt{3}/2) (M_{D2}/r^3) \cos I \{ 3 \sin(\varphi - 60^\circ) \cos \varphi + (\sqrt{3}/2) \} \end{aligned}$$

The magnetic moments, M_p , M_H , H_z , M_{D1} ($\equiv M_H$) and M_{D2} are 14.8, 6.60, 3.28, 6.60 and 2.84×10^8 oersted \cdot cm 3 respectively.

Relative locations of the sensor houses are determined so as to make the calculated effects of other sensors less than 0.1γ . In Fig. 20, OH, OD, OZ and OF are the sensor houses for the H , D , Z and F optical pumping magnetometers respectively. Calibration house 1 contains the sensor of the proton magnetometer, the DI-72 and two large coil systems, whereas calibration house 2 is provided for

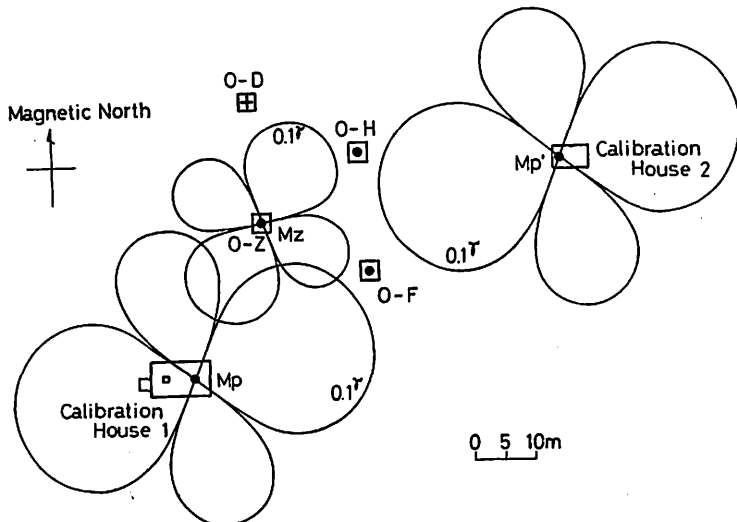


Fig. 22. Contours of 0.1γ for the H_y component of the disturbance fields produced by the magnetic moment M_p , M_z and M_p' . The D optical pumping magnetometer, laid in the OD house to detect the H_y component of the natural field, is clearly outside of their influence.

the calibration of such magnetometers that may produce external magnetic fields. Examples of the 0.1γ -contour line are shown in Fig. 22 for the H_y component produced by moments M_p and M_z . M_p' of calibration house 2 expresses the case that a similar proton magnetometer is laid in the house to be calibrated.



Fig. 23. Sensor houses of the KASMMER system viewed from the north.

Fig. 23 shows the view of the sensor houses seen from the north. Two small houses seen in the photograph are annexes to the sensor houses. The test house (not shown in the photograph) houses an astatic magnetometer and an optical pumping magnetometer for the measurement of material magnetism.

3.3 Sensor houses for the optical pumping magnetometer

The sensor houses, OH, OD, OZ and OF have the same structure mainly made of non-magnetic concrete blocks reinforced by brass rods. A house occupies approximately 11 m^2 , with a granite pillar at its center (Fig. 24).

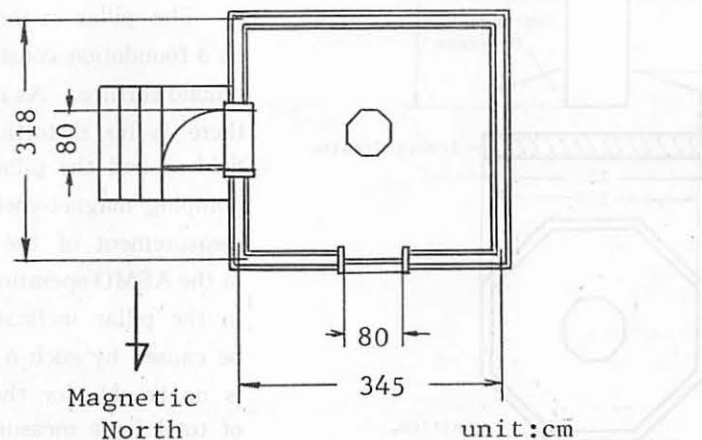


Fig. 24. Plan of sensor house OH, OD, OZ or OF.

The non-magnetic concrete block is made of white cement and small pieces of crushed granite of various sizes. The "Inadaishi", the commercial name of the granite produced at Inada near Kakioka, is a good building material with good non-magnetic properties. After testing samples from many stone pits at Inada, the most favorable pit was chosen to take the material for the houses and pillars. The magnetic susceptibility of the granite taken from the pit is 3×10^{-6} emu/cm³ at the most.

Instead of ordinary sands, gravels, and cements which include magnetic substances, fine and small pieces of granite and white cements are used to make concrete for the houses.

For the roof of the house, aluminium plates are used. Heat insulating materials are pasted onto concrete block walls, floor and ceiling. The outside of the wall is covered with aluminium sidings which contain heat-insulating glass wool.

The pillar's section is right octagon of 60 cm in diameter. The length of the pillars in houses OH, OD and OZ is 2.8 m of which nearly half is buried in the ground (Fig. 25). Its bottom is fixed on the octagonal non-magnetic concrete foundation reinforced by brass rods.

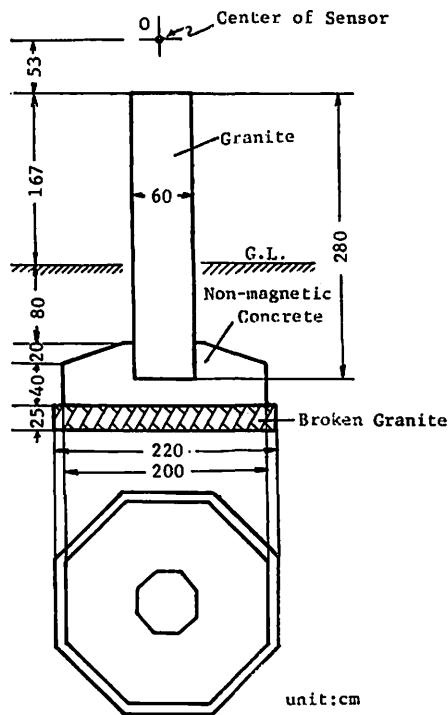


Fig. 25. Pillar in sensor house OH, OD, or OZ.

foundation reinforced by brass rods. The underground part of the pillar and the foundation form a magnetically hollow space which distorts the natural field above the ground. The distortion is estimated at a few gammas at the center of the magnetometer sensor (point O in Fig. 25).

The pillar in the house OF is laid on a foundation constructed just on the ground surface. As no soil is removed, there is no distortion in the natural field around the pillar. The F optical pumping magnetometer is used for the measurement of the total force except in the ASMO operation. A slight change in the pillar inclination, which might be caused by such a simple foundation, is no trouble for the routine operation of total force measurement.

Two different structures of the

pillars will give a possibility to examine the very local secular variation around the pillars.

3.4 Calibration house 1

Calibration house 1 is a tall rectangular non-magnetic house whose plan and vertical section are shown in Fig. 26. The lower part (up to 1.6 m from the ground) of the side wall is made of non-magnetic concrete reinforced by brass rods. On this, non-magnetic concrete blocks are laid up to a height of 5.6 m from the ground, reinforced by brass rods. The structures of its wall, ceiling and roof are almost the same as the sensor houses for the optical pumping magnetometer except for a part of the south wall. This part was initially an opening for carrying the

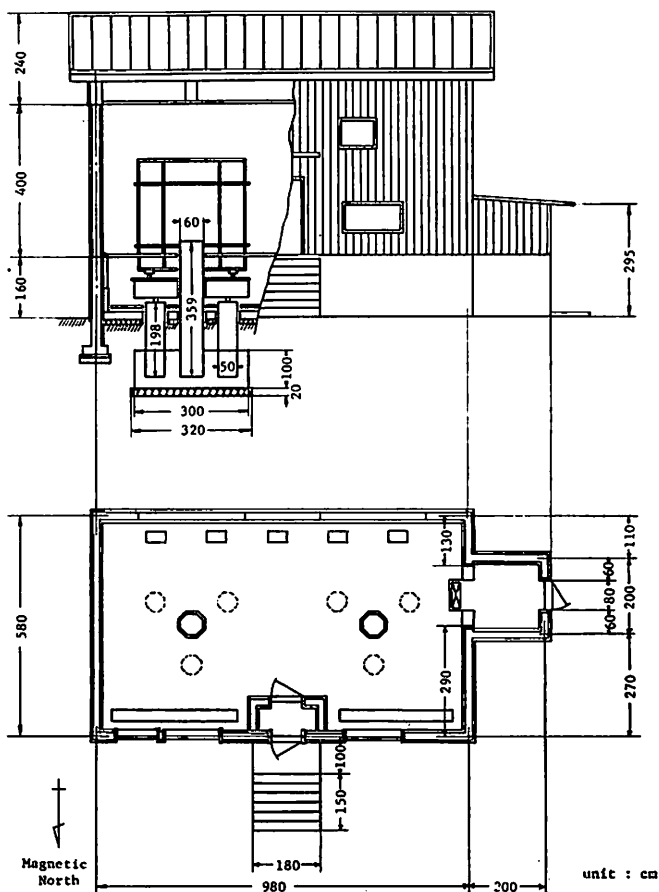


Fig. 26. Plan and vertical section of calibration house 1.

large coil systems into the house, and then closed by a wooden structure with similar covers as the other part.

The front door and four windows are set in the north wall; higher two windows are for the observation of the Polaris and lower two for the azimuth mark. Each of two large coil systems stands on three separate Inadaishi pillars (Fig. 26). A tall Inadaishi pillar is provided for installation of an instrument at the center of the coil system. Approximate dimensions of the pillars and foundations are shown in Fig. 26. The size of each foundation is a minimum for supporting the weight of the coil system and pillars with sufficient stability. This is because the field distortion has to be kept to a minimum as is described in Section 3.1. Thus, the distortion is estimated at less than a few gammas at the center of the coil system.

A second floor, 1.6 m high from the ground, gives easy access to the instrument laid at the center of the large coil system. The floor is mechanically insulated from the pillars and the coil system.

The DI-72 is laid at the center of the large coil system in the east side. The sensor of the proton magnetometer is hung from the ceiling over the DI-72.

Without an air-conditioner, the room temperature may exceed the limits for the DI-72 in hot and cold seasons, though the heat-insulating structure of the house slows down rapid changes. For the cold season, fifteen infrared lamps of 500 W are attached under the second floor. The nickel stem of the lamp is replaced by non-magnetic molybdenum. On-off of the lamps is automatically controlled by a thermostat. One-third of the total power, 2.5 kW, is sufficient to maintain the room temperature at 20°C during the cold season.

In a very hot season, a cooler is carried into the lean-to on the west side of the house. Running along the wall, the cool-air duct opens up near the ceiling.

A three-wheeled cart and 50 m-long track are provided for moving the cooler to a shelter at the end of the track when a magnetometer is operated. By the heat-insulating structure of the house, the room temperature is maintained well below the imposed temperature limit during the period of calibration measurement.

3.5 Other houses

Calibration house 2

This house is used for the calibration of such magnetometers that may disturb the measurement by the KASMMER instruments if operated in the west half of calibration house 1. For example, a proton magnetometer produces an intense external magnetic field at the time of polarizing, and then, it disturbs the operation of the KASMMER proton magnetometer or the DI-72 if their parallel measure-

ments are carried out in the same house. Placed in calibration house 2, its polarizing field will not disturb any sensor of the KASMMER system as is shown in Fig. 22. With floor space of approximately 21 m², the structure of the house is very similar to the sensor houses except three windows provided for the observation of the Polaris and the azimuth marks.

Two Inadaishi pillars stand on a non-magnetic concrete foundation which is constructed just on the ground surface in the house. Distortion in the natural field around the pillars is negligible. A portable optical pumping magnetometer is laid on a pillar for ready use.

Test house

This is a non-magnetic house of 9 m² with a basement. An astatic magnetometer is installed in a very deep niche in the basement, and an optical pumping magnetometer is laid on the ground-level floor. The sensor of the optical pumping magnetometer can be carried out from the house to examine extra-long or large materials outdoors.

Control house

This is made of concrete blocks. Fig. 27 shows the plan of the house and the arrangement of the KASMMER instruments in it.

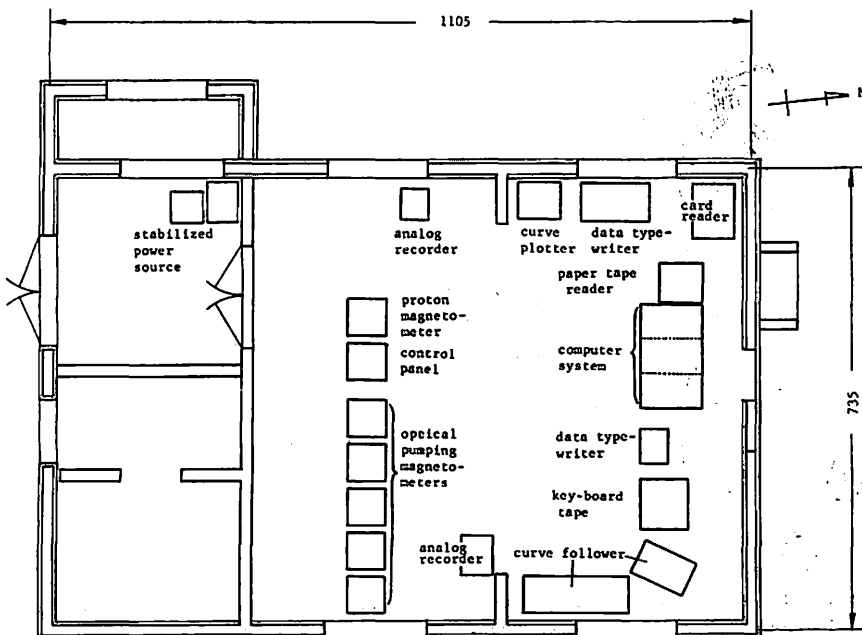


Fig. 27. Control house. (unit: cm)

3.6 Magnetic survey

Before the construction of the new ground, the distribution of the magnetic field was surveyed by Ochi (1970). During the period from October to December

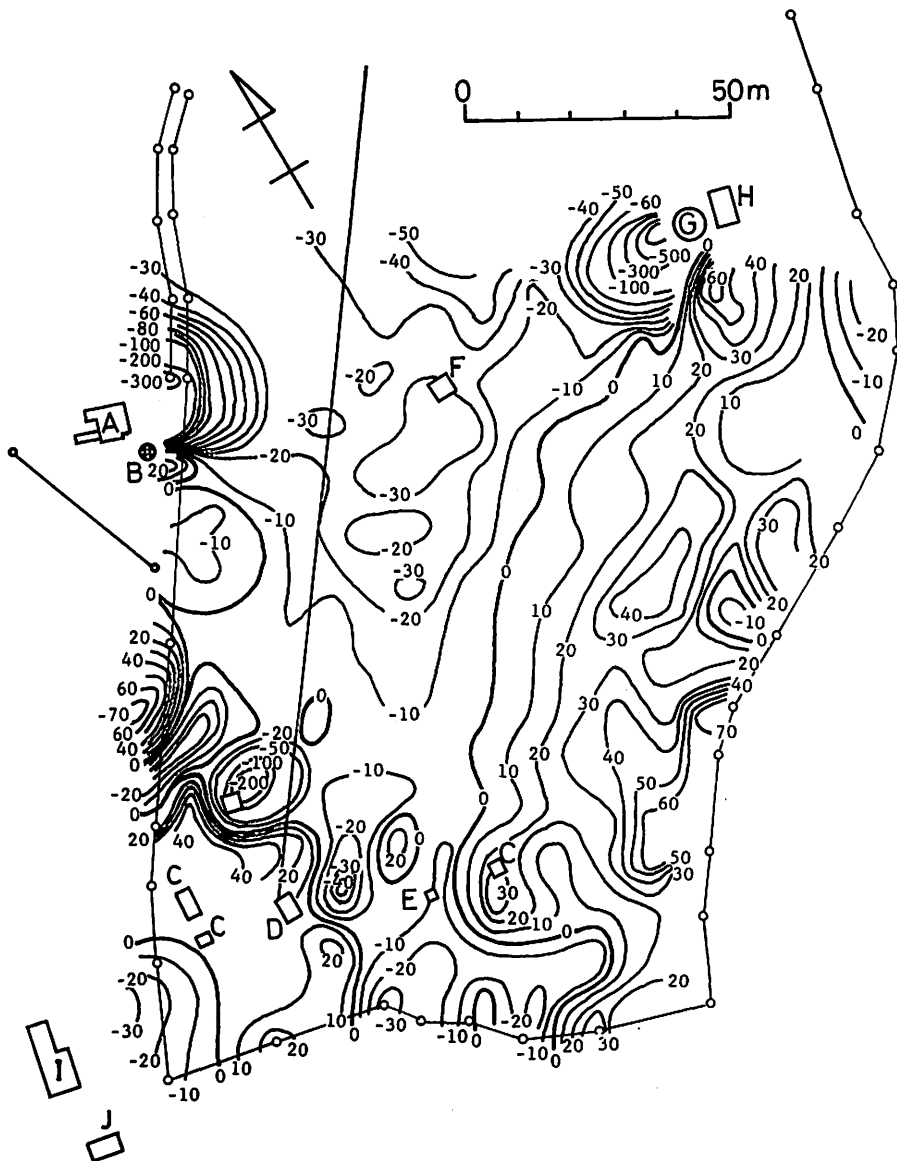


Fig. 28. Distribution of total force F in 1968 reproduced from Ochi's report. Contour lines are drawn at 10γ intervals. The figure attached to the contour line indicates the difference (in γ) from the value at the location of the routine absolute instrument.

1968, he measured total force F by a portable proton magnetometer at 10 m intervals, and declination D and dip I by a first-order GSI magnetometer at 20 m intervals. The distribution of F is reproduced in Fig. 28 which shows a rather complicated distribution due to the ground undulation and presence of buildings. Even in the central part, the gradient of the magnetic field exceeds $1 \gamma/m$.

After the construction of the new ground in the summer of 1970, second

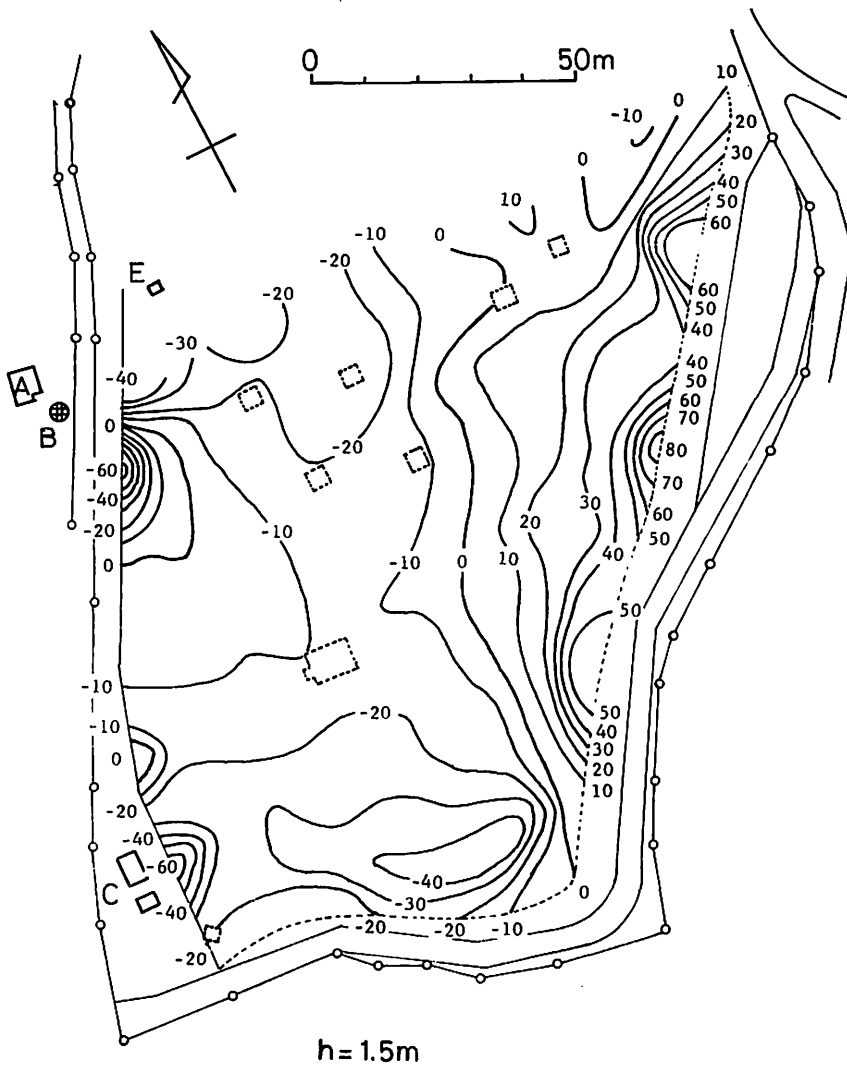


Fig. 29. Distribution of total force F in 1970 reproduced from Kurihara's report. Contour lines are drawn at 10γ intervals. The figure attached to the contour line indicates the difference (in γ) from the value at the location of the routine absolute instrument.

magnetic survey was conducted by Kurihara (1972). The same magnetometers were used again. All measurements were carried out at 10 m intervals. The distribution of F is similarly reproduced in Fig. 29. Anomaly in distribution pattern has been much reduced, at least in the central part of the ground. The locations of the sensor houses of the KASMMER system are shown by dotted rectangular figures, though they had not been built yet when the survey was carried out except the test house. Along the boundary of the new ground, anomalies still exist due to old buildings on the outside or the drop of level between the new ground and the low-lying farm fields. As is seen in the figure the influence of the boundary anomalies seems not to extend to the central part where the new sensor houses are built.

The same magnetic survey will be repeated periodically in future in order to watch the slow change in the distribution of the magnetic field.

Chapter 4. Operation and Test Result

4.1 Present state of KASMMER operation

Though the KASMMER system is very versatile, only routine observations and related tests have been carried out as of December 1972 since the installation in August 1972. Particularly the data acquisition system has been used only for primary data processing, though it facilitates calculation of data for further scientific analyses. Many programs are under preparation. The large coil system too has not been used yet. The following sections of this chapter will give the results on the routine operation and related tests. These are generally considered to be satisfactory.

4.2 Primary data processing for continuous operation of the optical pumping magnetometers

The BCD form outputs of the continuously operated four optical pumping magnetometers are sent to the computer system on line at 3-sec intervals. In routine operation, minute-values sampled at 00 second only are processed. The program of the primary data processing for the minute-value is as follows.

- 1) Judged from the apparent rate of change in the minute-value, very abnormal values are rejected.
- 2) Corrections of the instrumental parameters and the location differences, which are given by the calibration measurement and stored in the computer

memory, are added to the raw data of F , H , H_y and Z .

- 3) Other components, D , I , X and Y , are calculated from the corrected values of F , H , H_y and Z , as well as a stability factor A by the following equations:

$$D = \cos^{-1} (H_y/H) + D_0 - 60^\circ$$

* MAI SEI FUN CHI LISTING:
MONTH:12
DAY:09

HOUR:01
MINUTE:00 - 59

KAKIOKA GEOMAGNETIC DATA DEC. 09. 1972

H= 29600.0 Z= 34200.0 D= 6. I= 49 X= 29400.0 Y= 2900.00 F= 45400.0

	H	Z	D	I	X	Y	F	A
01H00M	494.1	411.6	21.37	-0.391	509.1	431.7	465.1	-0.162
01H01M	494.3	411.4	21.39	-0.396	509.3	431.9	465.3	0.157
01H02M	494.4	411.3	21.37	-0.421	509.4	431.7	465.1	-0.132
01H03M	494.4	411.7	21.37	-0.401	509.4	431.7	465.4	-0.134
01H04M	494.3	411.2	21.36	-0.404	509.3	431.6	465.2	0.208
01H05M	494.6	411.6	21.37	-0.421	509.6	431.7	465.4	-0.190
01H06M	494.8	411.3	21.38	-0.441	509.8	431.8	465.4	-0.095
01H07M	494.8	411.7	21.41	-0.421	509.8	432.1	465.7	-0.097
01H08M	494.8	411.5	21.42	-0.428	509.8	432.2	465.6	0.053
01H09M	494.9	412.0	21.44	-0.412	509.8	432.4	466.0	-0.089
01H10M	495.1	411.8	21.44	-0.431	510.0	432.4	466.0	-0.069
01H11M	495.2	411.8	21.45	-0.435	510.1	432.5	466.1	0.064
01H12M	495.3	412.2	21.45	-0.419	510.2	432.5	466.5	0.097
01H13M	495.4	412.1	21.45	-0.435	510.3	432.5	466.4	-0.092
01H14M	495.6	412.0	21.42	-0.455	510.6	432.3	466.4	-0.148
01H15M	495.7	412.5	21.44	-0.439	510.6	432.5	466.8	-0.191
01H16M	495.7	412.6	21.44	-0.432	510.6	432.5	466.9	-0.166
01H17M	495.7	412.0	21.43	-0.452	510.6	432.4	466.6	0.085
01H18M	495.7	412.0	21.45	-0.458	510.6	432.6	466.5	-0.114
01H19M	495.7	412.5	21.48	-0.432	510.6	432.8	466.9	-0.091
01H20M	495.7	412.2	21.51	-0.445	510.6	433.0	466.7	-0.065
01H21M	495.6	412.1	21.51	-0.442	510.5	433.1	466.6	0.076
01H22M	495.7	411.9	21.53	-0.458	510.5	433.3	466.5	0.061
01H23M	495.3	412.5	21.53	-0.399	510.1	433.2	466.8	0.171
01H24M	495.5	412.0	21.55	-0.445	510.3	433.4	466.4	-0.082
01H25M	495.4	412.4	21.57	-0.422	510.2	433.5	466.6	-0.119
01H26M	495.3	412.0	21.59	-0.438	510.1	433.7	466.2	-0.151
01H27M	495.2	412.0	21.62	-0.428	510.0	434.0	466.2	-0.086
01H28M	495.5	412.1	21.64	-0.452	510.2	434.2	466.3	-0.258
01H29M	495.7	412.2	21.65	-0.445	510.4	434.3	466.7	-0.065
01H30M	496.1	412.6	21.64	-0.453	510.8	434.2	467.2	-0.129
01H31M	496.4	413.0	21.63	-0.456	511.1	434.2	467.6	-0.228
01H32M	496.8	412.8	21.63	-0.483	511.5	434.3	467.8	-0.139
01H33M	496.9	413.2	21.63	-0.467	511.6	434.2	468.2	-0.107
01H34M	496.6	413.2	21.63	-0.450	511.3	434.2	468.0	-0.110
01H35M	496.6	412.7	21.65	-0.470	511.3	434.3	467.7	0.067
01H36M	496.5	412.9	21.68	-0.453	511.2	434.6	467.8	0.081
01H37M	496.6	412.8	21.70	-0.470	511.3	434.8	467.7	-0.108
01H38M	496.8	413.2	21.71	-0.457	511.5	434.9	468.2	0.058
01H39M	497.0	413.4	21.74	-0.457	511.6	435.2	468.5	0.076
01H40M	497.1	413.3	21.76	-0.474	511.7	435.4	468.4	-0.113
01H41M	497.1	413.7	21.77	-0.454	511.7	435.5	468.7	-0.115
01H42M	497.2	413.4	21.78	-0.477	511.8	435.6	468.5	-0.154
01H43M	497.1	413.6	21.81	-0.461	511.7	435.8	468.6	-0.140
01H44M	497.1	413.2	21.81	-0.474	511.7	435.8	468.4	0.061
01H45M	497.1	413.2	21.84	-0.474	511.6	436.1	468.4	0.061
01H46M	497.4	413.1	21.86	-0.510	511.9	436.3	468.3	-0.259
01H47M	497.2	413.5	21.88	-0.471	511.7	436.5	468.6	-0.130
01H48M	497.2	413.4	21.90	-0.471	511.7	436.6	468.6	-0.054
01H49M	497.4	413.4	21.91	-0.484	511.9	436.7	468.7	-0.086
01H50M	497.4	413.5	21.91	-0.477	511.9	436.7	468.8	-0.061
01H51M	497.6	413.8	21.92	-0.478	512.1	436.9	469.1	-0.119
01H52M	497.7	414.1	21.93	-0.468	512.1	436.9	469.4	-0.111
01H53M	497.7	413.6	21.92	-0.494	512.2	436.8	469.0	-0.133
01H54M	497.8	414.1	21.95	-0.478	512.2	437.1	469.4	-0.176
01H55M	497.9	414.1	21.98	-0.481	512.3	437.4	469.5	-0.142
01H56M	498.1	413.9	21.98	-0.501	512.5	437.4	469.5	-0.122
01H57M	498.1	414.4	22.01	-0.475	512.5	437.7	469.9	-0.099
01H58M	498.2	414.0	22.02	-0.498	512.6	437.7	469.7	-0.063
01H59M	498.2	413.8	22.03	-0.511	512.5	437.9	469.5	-0.112

Fig. 30. Hourly table of the minute-values.

$$I = \cos^{-1} (H/F)$$

$$X = H \cos D$$

$$Y = H \sin D$$

$$A = F - \sqrt{H^2 + Z^2}$$

where D_0 is a constant determined by calibration.

- 4) If any one of thus calculated components changes exceeding a given limit compared with the immediately preceding value, or if A exceeds a given limit, a special mark is attached to the value and an alarm lamp lights in the staff office.
- 5) Minute-values of H , Z , D , I , X , Y , F and A are stored in the magnetic disc memory.
- 6) Hourly mean values are calculated from minute-values and stored in the same memory.
- 7) Hourly table of the minute-value and daily table of the hourly mean value are typed out by the data typewriter.

MAI JI CHI LISTING:
MONTH: 10
DAY: 08

KAKIOKA

GEOMAGNETIC DATA

OCT. 08. 1972

H: 29600.0 Z: 34200.0 D: 6. I: 49 X: 29400.0 Y: 2900.0 F: 45400.0

	H	Z	D	I	X	Y	F	A	M	L	N
01	465.2	412.8	19.93	1.321	481.8	415.9	447.2	0.0	00	00	60
02	466.1	414.6	21.19	1.356	481.5	427.0	449.1	0.0	00	00	60
03	480.2	420.1	22.91	0.830	493.8	443.5	462.5	-0.0	00	00	60
04	496.2	427.3	24.77	0.271	507.9	461.5	478.4	-0.1	00	00	60
05	506.6	433.8	25.24	0.006	517.7	466.7	490.1	-0.1	00	00	60
06	508.4	433.7	24.06	-0.105	520.7	456.7	491.2	-0.0	00	00	60
07	504.8	431.5	22.52	-0.005	518.6	442.8	487.3	0.0	00	00	60
08	499.2	426.7	21.80	0.076	513.8	436.0	480.0	0.0	00	00	60
09	494.6	426.9	22.00	0.350	509.0	437.2	477.1	-0.0	00	00	60
10	494.7	431.2	22.06	0.554	509.1	437.8	480.4	0.0	01	00	60
11	495.0	432.5	22.10	0.602	509.3	438.2	481.6	0.0	00	00	60
12	493.9	432.6	22.21	0.668	508.1	438.9	481.0	0.0	00	00	60
13	494.1	433.4	22.23	0.701	508.2	439.1	481.7	0.0	00	00	60
14	494.9	434.1	22.10	0.689	509.2	438.1	482.8	0.0	00	00	60
15	495.7	434.4	21.92	0.654	510.2	436.6	483.4	-0.0	00	00	60
16	495.3	434.2	21.79	0.672	509.9	435.5	483.1	0.0	00	00	60
17	496.3	434.8	21.44	0.645	511.2	432.5	484.2	0.0	00	00	60
18	497.0	435.3	21.25	0.627	512.1	430.9	485.0	0.0	00	00	60
19	498.1	436.4	21.37	0.616	513.1	432.1	486.6	-0.0	00	00	60
20	498.5	435.2	21.22	0.537	513.7	430.9	486.0	0.0	00	00	60
21	502.3	435.9	21.01	0.355	517.6	429.4	489.0	0.0	00	00	60
22	504.2	435.0	20.57	0.208	519.9	425.8	489.6	0.0	00	00	60
23	499.5	428.6	19.76	0.157	516.1	418.3	481.7	0.0	00	00	60
24	491.5	420.9	19.06	0.237	508.7	411.3	470.6	0.1	00	00	60

Fig. 31. Daily table of the hourly mean values.

Figs. 30 and 31 show copies of an hourly table and a daily table, respectively. The force components H , Z , X , Y , F and A are expressed in γ , whereas angles D and I are in minute of arc. The constants given in the head line should be added to the values shown below. "MAI SEI FUN CHI" in the head title means the minute-value, and "MAI JI CHI" the hourly mean value. L and M in the daily table express the numbers of alarms issued for abnormal value of the components and for that of A , respectively, whereas N is the number of the minute-value adopted for the respective one hour. Data is stored in the disc memory in the same format for 8 hours for the hourly table and for 3 months for the daily table. They can be transferred to digital magnetic tape upon command.

The analog recorder continuously records analog outputs of four components, F , H , D and Z , monitoring the operation of optical pumping magnetometers. The D component is composed directly from the analog signals of H and H_y

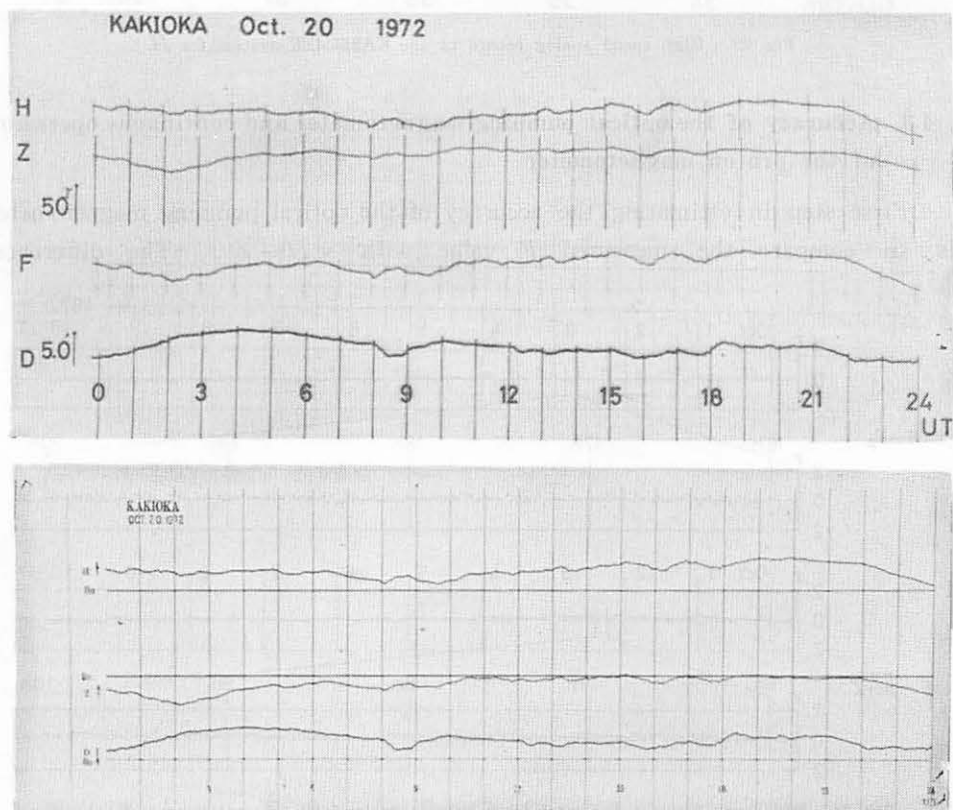


Fig. 32. Analog record of the KASMMER system with normal speed for a monitor (upper), and normal magnetogram of the bar-magnet variometers (lower).

through the differential amplifier (Fig. 6). Fig. 32 shows a part of the analog record for a day, together with the normal magnetogram of the bar-magnet variometers on the same day. High speed and high sensitivity record is available from another recorder. An example is shown in Fig. 33 for the H component. Small irregular fluctuations of about 0.03γ may include both the instrumental noise and artificial disturbances caused probably by the electric railways near Tokyo. They cannot be separated from each other on the record. This means also that neither noise exceeds 0.03γ .

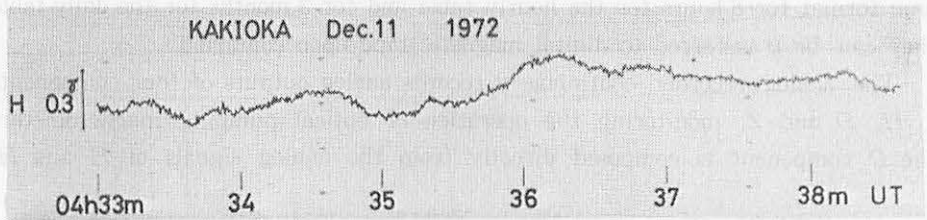


Fig. 33. High speed analog record of the KASMMER system for H .

4.3 Accuracy of the optical pumping magnetometer and continuous operation of the proton magnetometer

First step in estimating the accuracy of the optical pumping magnetometer is to compare the measured F value with $\sqrt{H^2+Z^2}$. The difference,

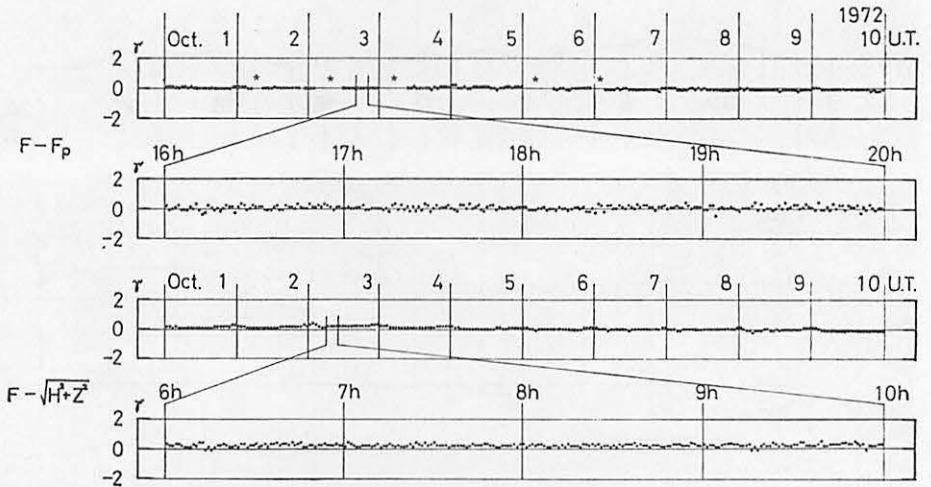


Fig. 34. Difference between the total force values obtained in different ways. F : by F optical pumping magnetometer, F_p : by proton magnetometer, $\sqrt{H^2+Z^2}$: by H and Z optical pumping magnetometers.

$A = F - \sqrt{H^2 + Z^2}$, is calculated in the primary data processing. Time variations of A are shown in Fig. 34 for 10 days. The occurrence frequency of the A value is given in Fig. 35 for 1440 minute-values. Instrumental parameters used in the primary data processing are unchanged for the whole period.

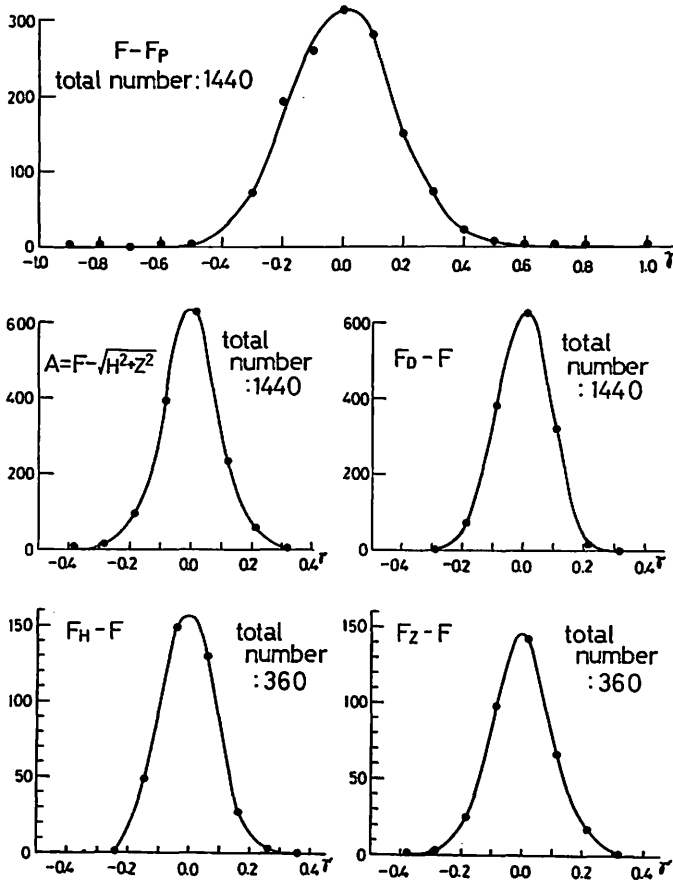


Fig. 35. Frequency distribution of the difference between the minute-values of the total force. F : by F optical pumping magnetometer, F_p : by proton magnetometer, $\sqrt{H^2 + Z^2}$: by H and Z optical pumping magnetometers, F_D , F_H , and F_Z : by D , H and Z optical pumping magnetometers, respectively, under no bias current.

As the figures show, almost all the A values are less than 0.1γ . This naturally leads us to consider that the real parameters of the three optical pumping magnetometers are unchanged, at least for the 10 days, and that the fluctuation in individual measured values is also less than 0.1γ . Because it is improbable that the three independent optical pumping magnetometers cause large independent

fluctuations in measured values satisfying the condition that the difference A be always nearly zero. A very remote possibility is that the three magnetometers cause such a parallel flow in measured values that results in $A=0$. To examine if our instruments have behaved in such a manner, the F value has to be compared with total force F_p simultaneously measured by the proton magnetometer.

The proton magnetometer can be operated automatically at intervals of 6-sec or a minute. Outputs in BCD form are sent to the computer system on line to calculate difference $F-F_p$. Hourly mean values of $F-F_p$ are shown in Fig. 34 for the same 10 days, together with minute-values for a part of the 10 days. In the period of the blank shown by asterisk, other tests of the system were carried out instead of the $F-F_p$ test. Frequency distribution of the difference value is also shown at the top of Fig. 35.

As the top row of Fig. 34 shows, difference $F-F_p$ is so constant during the period that the said possibility of the flow in F has to be discarded. Accordingly the flow in H or Z does not exist either. Considering the results of $F-F_p$ and $F-\sqrt{H^2+Z^2}$, the three optical pumping magnetometers for F , H and Z give satisfactory data with an accuracy of 0.1γ or so. This means also that the technique of the bias field is good for measuring the components.

The occurrence frequency of $F-F_p$ shown in Fig. 35 distributes over a wider range than A . This must be due to the fluctuation in individual measured values of F_p . The optical pumping magnetometer will give a more correct value for an instant field, provided that its instrumental parameter is determined by calibration. Considering the wider fluctuation of F_p , many simultaneous measurements of F

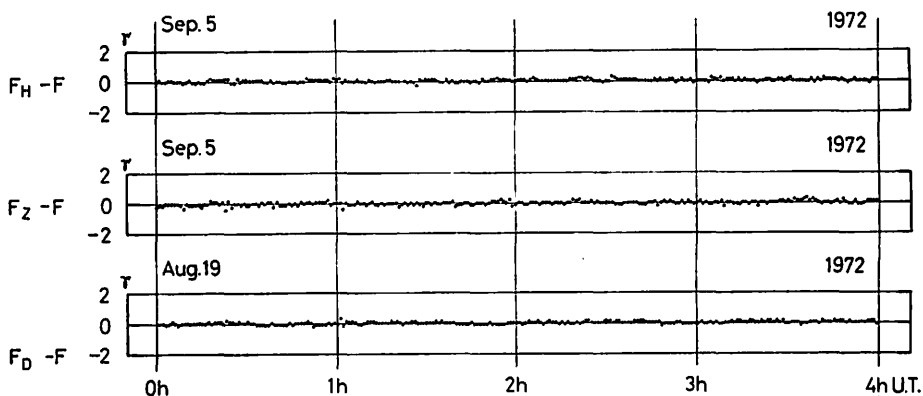


Fig. 36. Difference between the minute-values of the total force F (obtained by the F optical pumping magnetometer) and F_H , F_Z or F_D (obtained by respective component optical pumping magnetometers under no bias current).

and F_p have to be carried out for calibration.

The accuracy of the measured values of D or H_y is hardly estimated in the same way. Then, total force F_D , which is the value measured by the D optical pumping magnetometer under no bias field, is compared with the simultaneous values of F . An example of the time variation of $F_D - F$ is shown in Fig. 36. Occurrence frequency of the difference value is shown in Fig. 35 for 1440 minute-values which include the example shown in Fig. 36. The frequency distribution is very similar to that of the A value. So the D optical pumping magnetometer under no bias field is similarly precise. Provided that the technique of the bias field is as good as those for H and Z , the D optical pumping magnetometer will give the same accuracy for H_y or D .

Similar differences $F_H - F$ and $F_Z - F$ are also shown in Figs. 35 and 36. F_H and F_Z are the total force measured by the H and the Z optical pumping magnetometer respectively under no bias field. Differences $F_H - F$, $F_Z - F$, $F_p - F$ and A are all very similar. This again indicates that the four optical pumping magnetometers are similarly precise.

Hourly mean values obtained by the optical pumping magnetometers are far

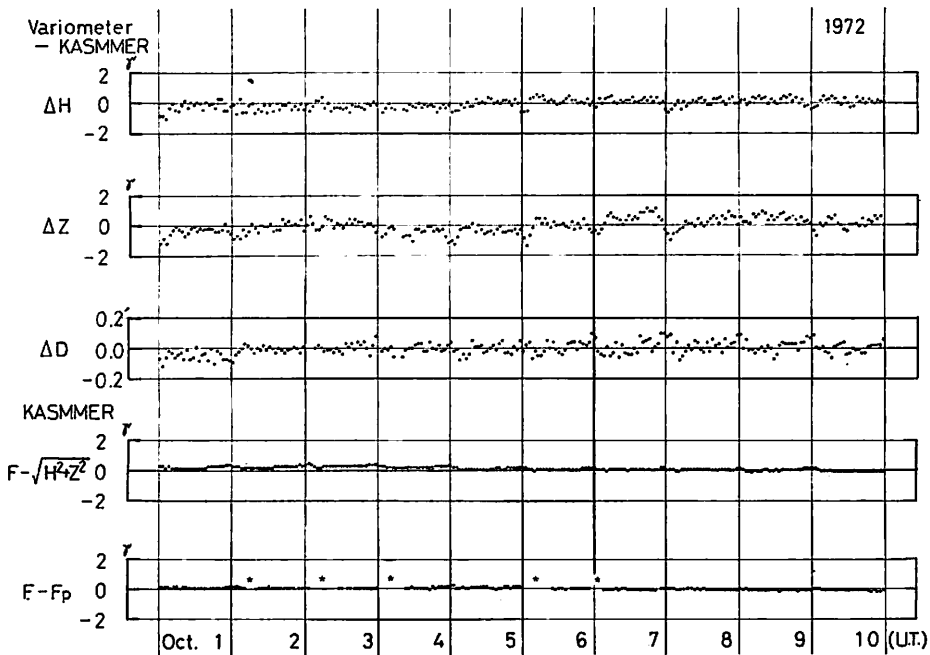


Fig. 37. Comparison of data between that hand-scaled from normal magnetograms and that of the present KASMMER system.

better than those obtained by the classical system of bar-magnet variometers in precision. Fig. 37 shows a comparison of the data. First three rows of the figure show differences ΔH , ΔZ and ΔD in the hourly mean values of the three components H , Z and D between two systems. Fluctuations in these rows should be compared with the last two rows which are the same ones as are given in Fig. 34. These fluctuations of ΔH , ΔZ and ΔD must be due to those in the variometer system. Their most part may depend on the hand-scaling, because an error of mere 0.1 mm on the magnetogram amounts approximately to 0.3γ . Unstability of the base-line value also assists the fluctuation, particularly for relatively long-period terms such as diurnal variation. Diurnal changes in ambient conditions could cause diurnal variation in instrumental error in any optical pumping magnetometer. Fig. 38 shows the mean diurnal variation of $F-F_p$ in a much magnified scale for

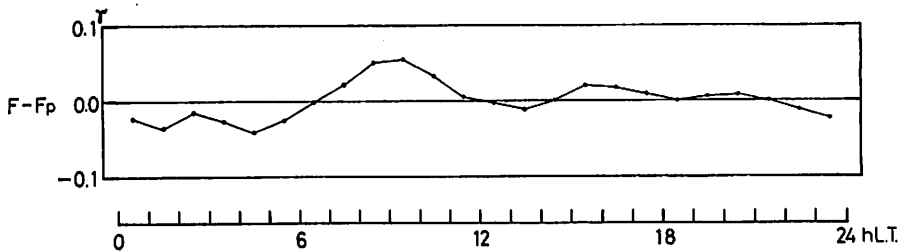


Fig. 38. Diurnal variation of the difference $F-F_p$ shown in a magnified scale (see Fig. 34).

15 days. Its significance is not clear, but a systematic variation of small amplitudes is seen. A possible cause of the variation is the change in the room temperature around the sensor of the optical pumping magnetometer. The amplitude of about 0.05γ is so small that there is practically no influence upon the accuracy of the measured value of the optical pumping magnetometer.

4.4 Calibration measurement

The measurement of $F-F_p$ described in the preceding section simply gives the calibration of the F optical pumping magnetometer. Fig. 39 shows daily mean values of $F-F_p$ from September 1 to October 12, 1972. The instrumental

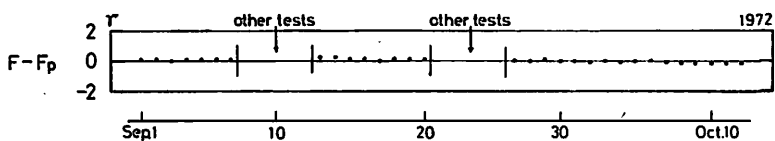


Fig. 39. Difference $F-F_p$ for daily mean values (see Fig. 34).

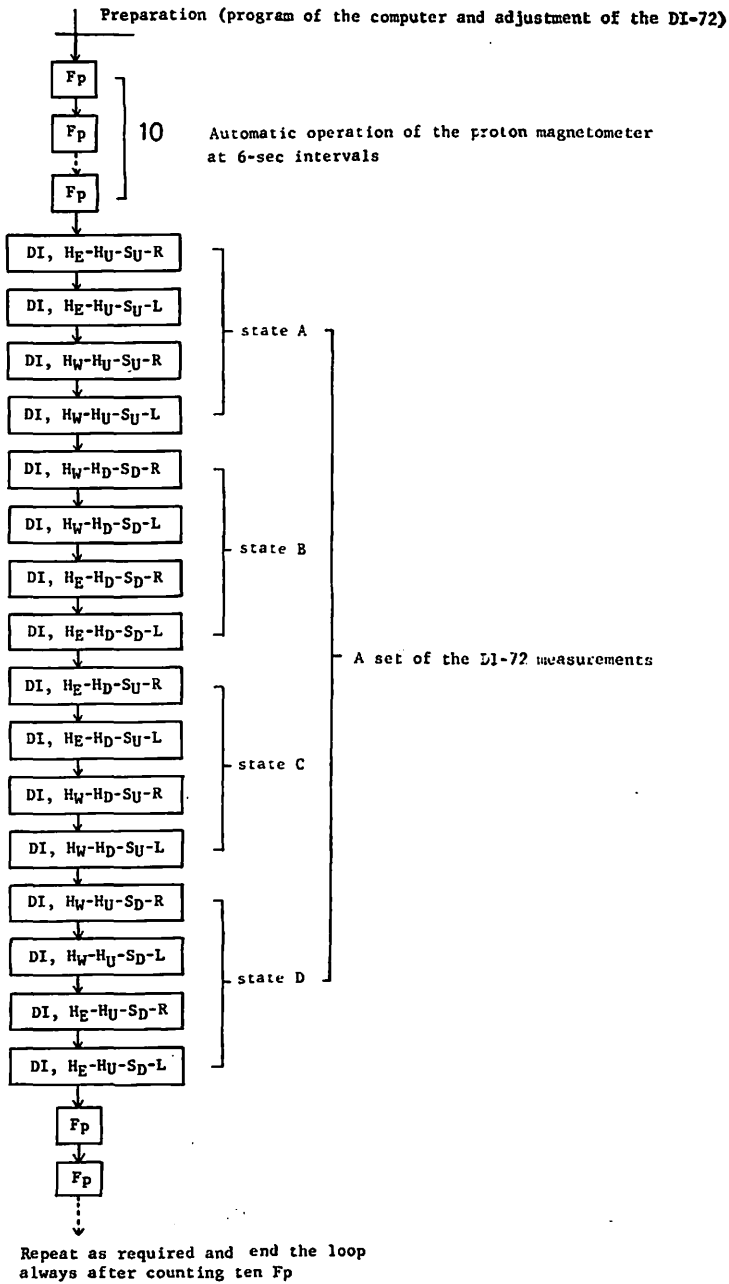


Fig. 40. A prepared procedure for the calibration measurement.

parameter of the optical pumping magnetometer used in the calculation is unchanged throughout the whole period. In the blank period and after October 13, other tests of the system were carried out so frequently that the data of $F-F_p$ was not enough to show the daily mean value.

As the figure shows, the real instrumental parameter to be calibrated by the measurement is practically constant for this period of longer than 40 days. The constancy of better than $0.1 \gamma/\text{week}$ aimed at in the planning has been attained, at least for this period.

For the calibration of the other component optical pumping magnetometers, more complicated procedure is necessary because the DI-72 is operated manually. One set of measurements by the DI-72 consists of 16 elements (Section 2.7) which give 4 values for each of declination D and dip I . Each component of the field is calculated from these values of D and I and the F_p values measured by the proton magnetometer. A prepared program of the calibration procedure is shown in Fig. 40.

When each element of the measurement shown in the figure is performed, simultaneous outputs of the four optical pumping magnetometers are stored in the computer automatically for the element of F_p , and upon command, for D and I . The simultaneous values of F , H , Z , D , I , X , Y and A are calculated and stored in the same way as the primary data processing.

The measured values of F_p are also stored automatically. On the other hand, the readings of the DI-72 are fed into the computer through the data typewriter when one series of measurements is completed. From the F_p values and the readings of the DI-72, each component of the field is calculated in the computer, where the time variation of the field is corrected by using the said simultaneous values obtained by the optical pumping magnetometer for each element. Then, the differences for each component of the field between the values obtained by the optical pumping magnetometers and those by the calibration system are calculated. A set of the DI-72 measurements together with the preceding and following F_p measurements gives 4 values of the difference for each component. A series of calibration measurements of n sets will give $N (=4n)$ values.

In order to estimate the precision of the DI-72, the fluctuation in individual measured values is examined. Using the said difference in D or I between the optical pumping magnetometer and the DI-72, the frequency distribution of the deviation of individual values from the mean of 4 values in a set is calculated for 37 sets ($n=37$, $N=148$) and shown in Fig. 41. The variance is $(0.018')^2$ for D or $(0.013')^2$ for I . Considering that measurement is made in 0.1γ increment for

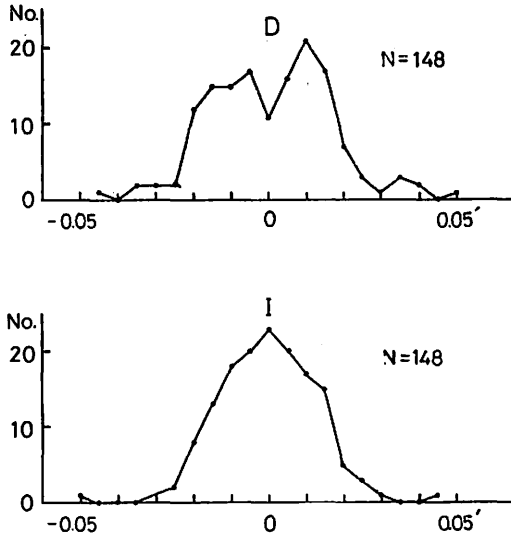


Fig. 41. Frequency distribution of the individual deviation of the declination value (upper) and the dip value (lower) measured by the DI-72.

the optical pumping magnetometer or $1'' (=0.017')$ for the DI-72, these small variances show the very good precision of the DI-72. A very small systematic deviation between different positions of the search coil (Section 2.7) is found in the frequency distribution for D . It is estimated to be $\pm 0.015'$. The shown distribution is the corrected one. For the purpose of calibration, it will be cancelled out by averaging the measured values in the different 4 states. No such systematic deviation is found for I .

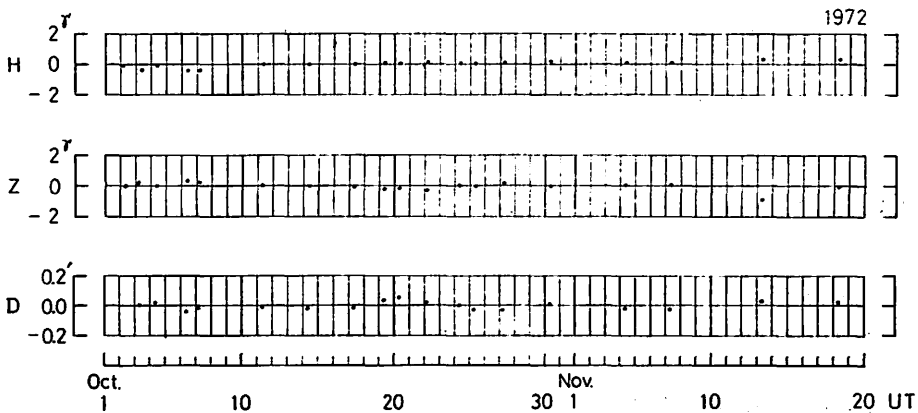


Fig. 42. Result of the calibration measurement.

Fig. 42 shows the result of the calibration measurement for the components. Time change of the difference is given for components H , Z and D . During the whole period, the instrumental parameters of the optical pumping magnetometer used in the calculation are unchanged. Fluctuations in the difference are a little larger than those of $F-F_p$. This may partly be due to the small number of the sets in a calibration measurement. Further examination on the change in the real parameter of the component optical pumping magnetometer will be carried out using larger numbers of sets for the DI-72 measurement. It seems to be better at the present to employ the mean value of the difference to determine the instrumental parameter, which is not so much changed in any way from the value determined at the beginning.

The dip and the declination measured by the DI-72 are compared with the dip value calculated from the horizontal and vertical components measured by the vector proton magnetometer MO-P, and with the declination measured by the A-56, respectively. Fig. 43 shows the difference obtained by weekly comparison

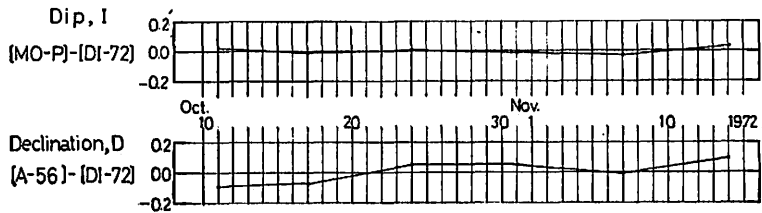


Fig. 43. Comparison of the DI-72 with the MO-P for the dip and with the A-56 for the declination.

measurements. Very small change in the difference in the dip indicates that both of the MO-P and the DI-72 are sufficiently accurate. On the other hand the difference in the declination changes over a wider range. As the A-56 seems to be less accurate than the present DI-72 (see Appendix), there is not much use for further examination.

4.5 ASMO method

The KASMMER system can utilize anytime the ASMO method to measure each component of the field. The sensing element of the F optical pumping magnetometer is laid at the center of two orthogonal Helmholtz coil pairs (Fig. 4).

One cycle of the ASMO measurement consists of 6 elements of measurement, F , F_+^D , F_-^D , F_+^I , F_-^I and F , which are performed automatically at 3-sec intervals

in the order named. The cycle of measurement starts upon command, and repeats continuously or once a minute as is desired. Data is processed automatically in the computer system.

Test operation of the method has been carried out for several days. Fig. 44 is an example of the result which shows the difference between the values obtained by the ASMO method, H_A , Z_A and D_A , and the simultaneous values obtained by

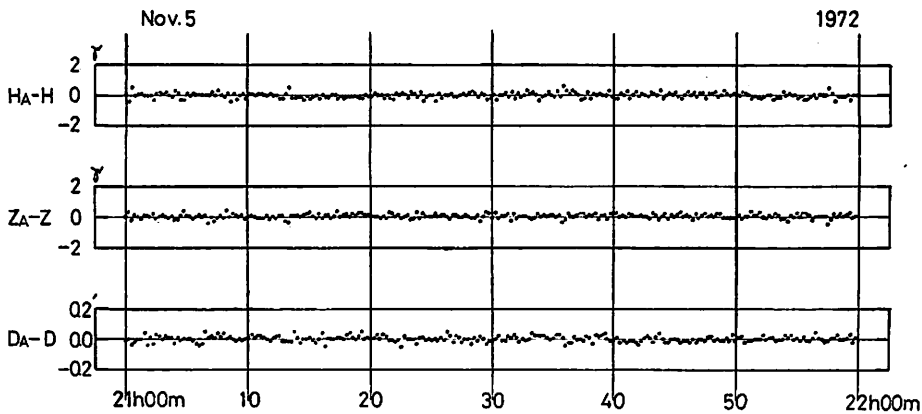


Fig. 44. Comparison of the ASMO method (H_A , Z_A and D_A) with the routine data obtained by the component optical pumping magnetometers (H , Z and D).

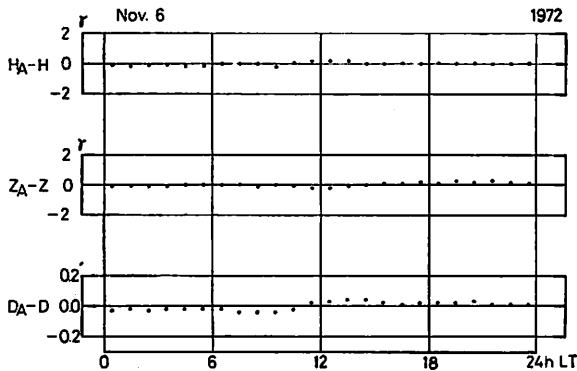


Fig. 45. Hourly mean values of the difference between the ASMO method and the component optical pumping magnetometers.

individual component optical pumping magnetometers, H , Z and D . Fig. 45 shows the same difference in hourly mean value for a day. Judging from the results, the ASMO method will give sufficiently accurate values to supplement the routine operation of the optical pumping magnetometers.

4.6 Semi-automatic digitization of analog record and reproduction of magnetogram from digital data

Semi-automatic digitization of analog record has been examined using magnetograms and the curve follower. The observer manipulates the tracer only along the ordinate to follow the trace of the magnetogram mounted on the deck of the device (Section 2.9). The coordinates are digitized automatically, and digital data is processed in the computer system. Instantaneous values of the magnetic field are calculated at intervals of a given time and stored in the computer. Hourly mean values are calculated from the instantaneous values. This technique has been tried on ordinary magnetograms obtained by the classical variometer system of Kakioka.

An example of the test result for a day is given in Fig. 46 which shows the differences in the hourly mean value between thus calculated values and those

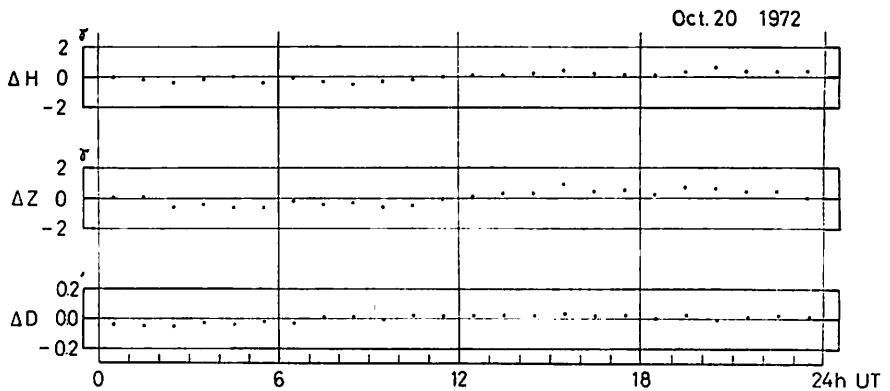


Fig. 46. Comparison of the semi-automatic digitization of the normal magnetogram (shown in the lower half of Fig. 32) with the routine data obtained by the optical pumping magnetometers.

obtained by routine operation of the optical pumping magnetometer. The differences are not so large in general. This technique of semi-automatic digitization seems to have the same preciseness as the usual hand-scaling, at least for hourly mean values.

From the instantaneous values stored in the computer, an analog record can be made by the curve plotter. Fig. 47 shows the "magnetogram" thus made for the same day. This magnetogram should be compared with the original one shown in Fig. 32.

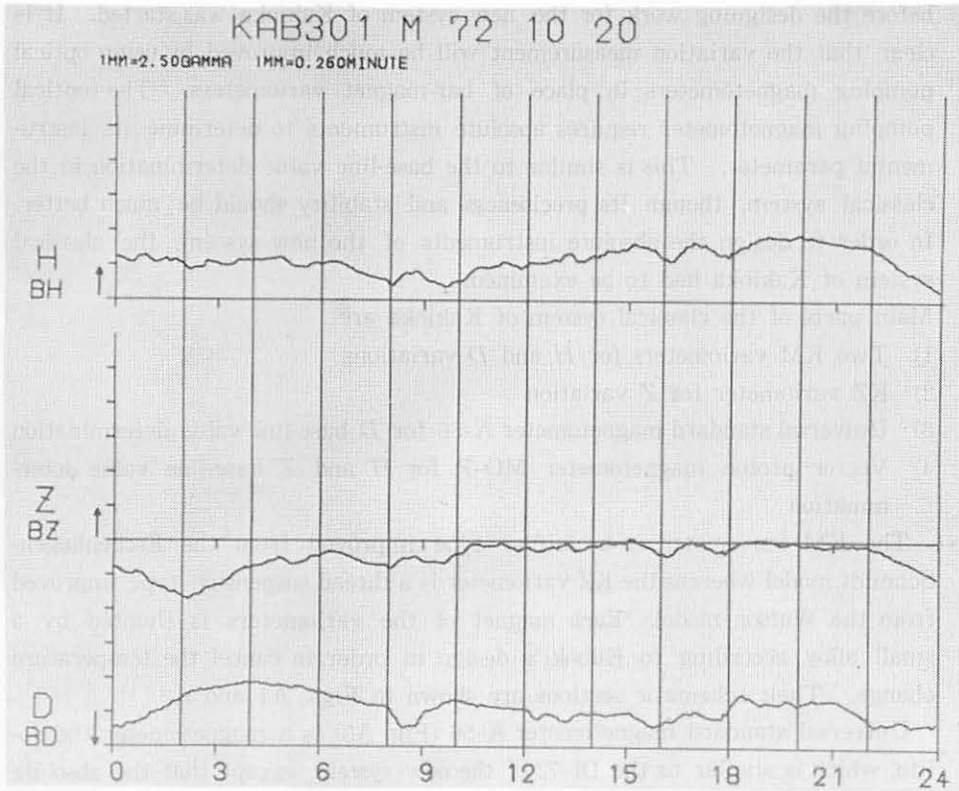


Fig. 47. A "magnetogram" made through the curve plotter from the digital values obtained by the semi-automatic digitization of the normal magnetogram shown in the lower half of Fig. 32.

Acknowledgements:—We would like to thank all staffs of the Kakioka Magnetic Observatory for their help in the construction and the test of the present system, particularly the Research Section for assistance in the preparation of this paper. Main instruments of the system were manufactured by Nihon Electric Co., Sokkisha Co., and Takeda Riken Industry Co. We are very grateful to the companies for their endeavor to improve the related technique.

Appendix

Accuracy of the base-line value determined by the A-56 and the vector proton magnetometer MO-P in the classical system of magnetic observation at Kakioka

1. Accuracy of the geomagnetic data obtained by the classical system was reviewed

before the designing work for the new system of Kakioka was started. It is clear that the variation measurement will be much improved by using optical pumping magnetometers in place of bar-magnet variometers. The optical pumping magnetometer requires absolute instruments to determine its instrumental parameter. This is similar to the base-line value determination in the classical system, though its preciseness and stability should be much better. In order to design the absolute instruments of the new system, the classical system of Kakioka had to be examined.

2. Main parts of the classical system of Kakioka are

- 1) Two KM variometers for H and D variations
- 2) KZ variometer for Z variation
- 3) Universal standard magnetometer A-56 for D base-line value determination
- 4) Vector proton magnetometer MO-P for H and Z base-line value determination

The KM variometer is a unifilar type improved from the Eschenhagen-Schmidt model whereas the KZ variometer is a thread suspension type improved from the Watson model. Each magnet of the variometers is shunted by a small alloy according to Kuboki's design in order to cancel the temperature change. Their schematic sections are shown in Figs. A1 and A2.

Universal standard magnetometer A-56 (Fig. A3) is a magnetometer theodolite, which is similar to the DI-72 of the new system, except that the absolute dimensions of its Helmholtz coil have been measured to 1μ , and that its search coil is directly used to obtain the field direction. The Helmholtz coil can create a known magnetic field in any direction, and the direction of the vector sum of the coil field and the geomagnetic field is measured by means of the search coil on rotation. The AC signal of the search coil is amplified and detected. Any component of the geomagnetic field can be calculated from combination of a few measurements in different, suitable coil fields. Before the vector proton magnetometer was installed at Kakioka, the base-line value determination had been carried out by the A-56 for all components. At the present, however, it determines only D base-line value.

Vector proton magnetometer MO-P is very similar to the Nelson model. It can give the values of H and Z , as well as F .

A sine-galvanometer H-56 (Fig. A4), whose Helmholtz coil is the same as the A-56, is provided to supplement the base-line determination. Second system of variometers, which similarly consists of two KM and one KZ, is also operated continuously.

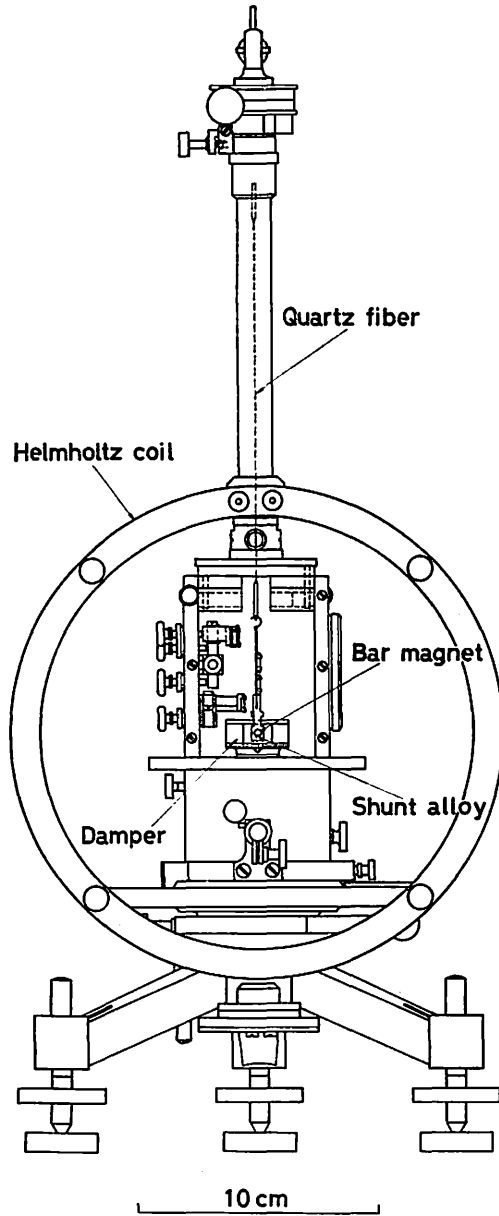


Fig. A1. KM variometer for H or D .

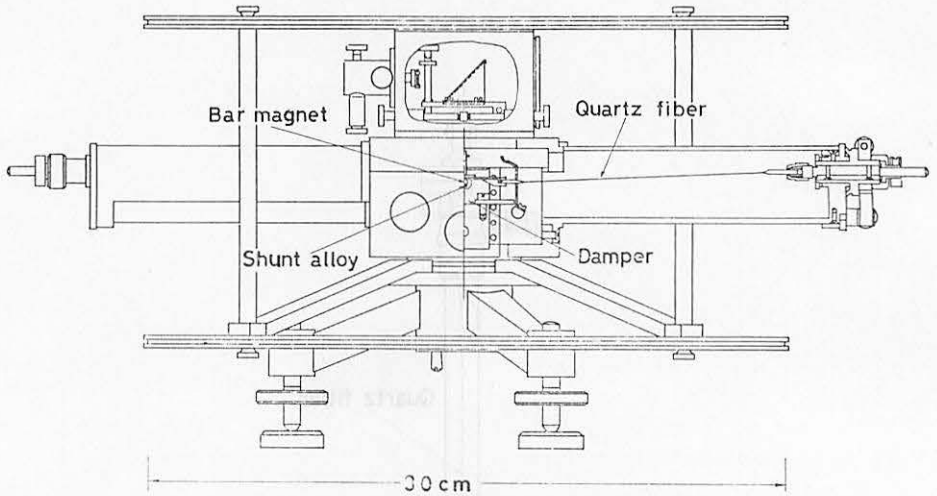


Fig. A2. KZ variometer for Z.



Fig. A3. Universal standard magnetometer A-56.

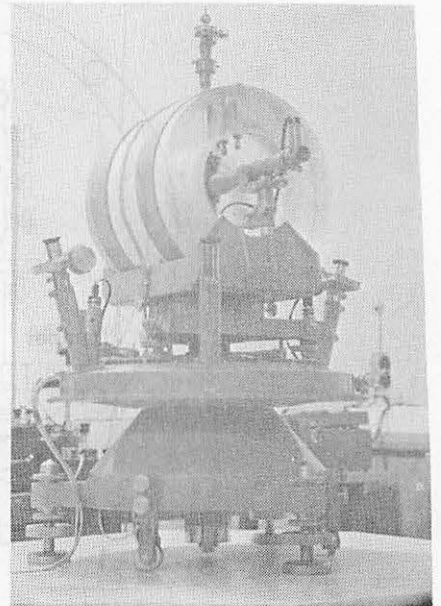


Fig. A4. Sine-galvanometer H-56.

3. Absolute measurements by the A-56 are carried out every other week. Under no current of the Helmholtz coil, the AC output of the search coil on rotation is amplified and detected. Watching the detected signal, the direction of the

rotation axis of the search coil is changed until the signal disappears. Then the direction is read to 1" from the graduated circle. The procedure of repeated measurements at 180°-turned positions for elimination of errors is the same as with ordinary theodolites. It gives the D value of the geomagnetic field from which the base-line value of the magnetogram is determined. One absolute measurement in a day consists of 4 measurements which give 4 base-line values, D_i ($i=1, 2, 3, 4$). The variance σ_D^2 calculated from the data of 1971 is,

$$\sigma_D^2 = \text{mean of } \sum_{i=1}^n (D_i - \bar{D})^2 / (n-1) = (2.93'')^2 \quad (n=4)$$

From the value of σ_D , the factor of the 95% confidence interval,

$$(\bar{D} - 1.96 \sigma_D / \sqrt{n}, \quad \bar{D} + 1.96 \sigma_D / \sqrt{n})$$

is given as follows:

$$1.96 \sigma_D / \sqrt{n} = 2.87''$$

The preciseness of the D base-line value determination is approximately 3". This does not necessarily express the accuracy of the A-56 itself, because this includes unstability of the variometer and errors on the magnetogram scaling. It is also to be noted that this does not necessarily mean the accuracy in absolute value but does mean the relative precision, though due considerations have been given to the instrument construction and the measurement procedure. These points will be discussed later in subparagraph 9.

4. Absolute measurements by the MO-P are carried out once a week. One absolute measurement in a day gives 10 base-line values for each of H and Z . The variances σ_H^2 and σ_Z^2 are calculated similarly for the data of 1971 as follows:

$$\sigma_H^2 = \text{mean of } \sum_{i=1}^n (H_i - \bar{H})^2 / (n-1) = (0.199 \gamma)^2 \quad (n=10)$$

$$\sigma_Z^2 = \text{mean of } \sum_{i=1}^n (Z_i - \bar{Z})^2 / (n-1) = (0.206 \gamma)^2 \quad (n=10)$$

The values,

$$1.96 \sigma_H \sqrt{n} = 0.123 \gamma \quad \text{for } H$$

$$1.96 \sigma_Z \sqrt{n} = 0.128 \gamma \quad \text{for } Z$$

give the factors of the 95% confidence interval,

$$(\bar{H} - 1.96 \sigma_H / \sqrt{n}, \quad \bar{H} + 1.96 \sigma_H / \sqrt{n})$$

or

$$(\bar{Z} - 1.96 \sigma_Z / \sqrt{n}, \quad \bar{Z} + 1.96 \sigma_Z / \sqrt{n})$$

The preciseness of the base-line value determination is considered to be $0.1-0.2\gamma$ in H or Z . If the value of the gyro-magnetic ratio is known, the proton magnetometer is believed to give the absolute value of the magnetic field. Nevertheless, there seems to be some questions to be studied on the point, which will be discussed later again.

5. σ_H or σ_Z includes the unstability of the variometer and errors on the magnetogram scaling. In order to estimate the precision of the MO-P itself, its values are compared with those obtained by an optical pumping magnetometer for total field intensity F ignoring the difference in absolute value. During a short time for the comparison, the optical pumping magnetometer would be stable and would give practically no fluctuation. From the simultaneous measurements, the variance σ_F^2 for the difference in F is given as follows:

$$\sigma_F^2 = (0.106\gamma)^2 \quad \text{for Proton - OPM}$$

When the values obtained by the optical pumping magnetometer are replaced by those measured from the magnetogram of the variometer system, the similar variance σ_V^2 is much increased as follows:

$$\sigma_V^2 = (0.293\gamma)^2 \quad \text{for Proton - Variometer}$$

The preciseness is clearly lowered when the variometer system is used. The value 0.2γ of σ_H or σ_Z is believed to be due to the errors on the side of the variometer system. The value 0.3 of σ_V is larger than σ_H or σ_Z because of the use of both H and Z on the variometer side. The proton magnetometer MO-P itself will give a precision of 0.1γ or so as is shown in σ_F .

6. σ_D is approximately $3''$ which corresponds to 0.43γ in the field intensity. This value exceeds 0.2γ which is the precision of the variometer side in H or Z . The variometer for D is far more simple than that for H or Z . Since the variometer side is not responsible for increased fluctuations the value 0.43γ of σ_D is mainly due to the A-56. Though the precision had surpassed our initial aim of $3''$ in direction or 0.5γ in field intensity, the cause of the fluctuation was investigated before designing the new system and two possible causes were found. One was the amplifier for the search coil signal, and the other was the play in the rotation axis of the search coil.
7. AC signals of the search coil on rotation are detected and amplified. The noise of conventional amplifiers appears to be larger than 0.1γ . When used for routine operations, our amplifier for the A-56 was fortunately the best among many kinds of amplifiers for magnetometer theodolites which we could test. Nevertheless the noise from the amplifier may cause a part of the

fluctuation expressed by σ_D . A new type of amplifier has been designed by Kuboki (Section 2.7) for the A-56 and the new system.

8. More serious problem than the amplifier was the play in the rotation axis of the search coil. The search coil has to be rotated in order to act as a detector of the DC field, inevitably requiring a clearance between the bearing and the axis. Since the precision was much improved when the clearance was much decreased until the search coil could barely rotate, the most part of σ_D of 3" must be due to the clearance. However the operations with the decreased clearance have to be much limited in number. Otherwise, the bearing will be worn out quickly. The precision of 3" will be the limit of this kind of magnetometer theodolite using the search coil directly.
9. The clearance of the bearing may influence the absolute value of the measured direction, particularly for dip I . With a clearance present, the direction of the rotation axis of the search coil may deflect in the bearing towards one direction due to the gravity notwithstanding the turned positions in a vertical plane. This causes an error in the absolute value of I . On the other hand, there seems to be no influence upon D , because the gravity acts evenly for the D measurement.

If there is something which influences the absolute value of D , material magnetism of the instrument may be the most possible one. Materials of the A-56 were carefully tested before its construction to make the magnetic field at its center below 0.1γ . So, the precision of 3" or 0.5γ quoted in subparagraph 3 above is really the degree of accuracy. If a better accuracy is aimed at, the stray magnetic field has to be made much smaller, because it may increase after a long time. It is not so easy to reduce the stray magnetic field, including all of magnetic induction, residual magnetism and currents in the metal, to below 0.1γ .

10. In theory, absolute values of the field intensity measured by the proton magnetometer are considered to be correct, except γ_p values. However, various instruments give different values for the same field intensity. The instrumental difference of 34 proton magnetometers of various types tested at Kakioka with the MO-P as the standard varied from -0.8γ to $+3.4\gamma$.

The most probable cause of the difference is again material magnetism. Residual magnetism is naturally expected of any detector because of the strong magnetic field impressed upon it to polarize. If the field of the residual magnetism is parallel to the polarizing field which is generally perpendicular to the field to be measured, the measured total intensity will not be affected

by the field of the residual magnetism. This is true generally in the first approximation. In actual instruments, the magnetization of the detector is not always strictly parallel to the polarizing field. In order to obtain the true absolute value of the field intensity, it is necessary to null the errors, for example, by reversing the polarizing current or turning the detector through 180° , besides, exclusion of magnetic materials from the detector.

11. It is to be noted that the measured value of the proton magnetometer slightly depends upon the temperature of the water in the detector. Temperature coefficients have been measured for 5 detectors. These are approximately -0.012 , -0.014 , -0.001 , -0.015 and $+0.006 \gamma/^\circ\text{C}$ from 0° to 80°C .
12. The A-56 is an absolute instrument for all the components. The MO-P is compared with it and with the sine-galvanometer H-56. Mean differences of the simultaneous measured values are, respectively,

$$\left. \begin{aligned} [\text{A-56}] - [\text{MO-P}] &= 0.1 \gamma \\ [\text{H-56}] - [\text{MO-P}] &= -0.2 \gamma \end{aligned} \right\} \text{ for } H$$

The values of the A-56 are those obtained in the situation of the decreased clearance of the bearing. So they are much more precise than those of the routine operation in both the absolute value and the fluctuation. For γ_p , $2.67513 \times 10^4 \text{ sec}^{-1} \text{ gauss}^{-1}$ is used. The difference values will give an idea of the absolute accuracy of individual instruments.

References

- Allredge, L. R. (1960): A Proposed Automatic Standard Magnetic Observatory. *J. Geophys. Res.*, **65**, 3777-3786.
- Bloom, A. L.: Principles of Operation of the Rubidium Vapor Magnetometer. *Appl. Opt.*, **1**, 61-68.
- Kuboki, T. (1968): A Study for Temperature Compensation of Magnetic Variometer by Means of Magnetic Shunt Alloy and Stabilization of Variometer. Doctorate Thesis, Tohoku University.
- Kurihara, T. (1972): Magnetic Anomaly and Its Change in the Proposed Site of New Standard Magnetometer in the Kakioka Magnetic Observatory. *Mem. Kakioka Magn. Obs.*, **14**, No. 2, 39-56.
- Ochi, K. (1970): Result of the Magnetic Survey in the Kakioka Magnetic Observatory Ground in 1968. *Mem. Kakioka Magn. Obs.*, **13**, No. 2, 31-48.
- Sano, Y. (1971): A Measuring Method of Magnetic Field Component with Optical Pumping Magnetometer and Its Error and Stability Related to the Compensating Field. *Mem. Kakioka Magn. Obs.*, **14**, No. 1, 19-38.
- Tsubokawa, I. (1951a): *G. S. I. Precise (First Order) Magnetometer*. Sakkisha Ltd. 390 Mishukumachi Setagayaku, Tokyo.

- Tsubokawa, I. (1951b): Theory of Electromagnetic Magnetometer Using a Rotating Coil-detector. *Bull. Geogr. Surv. Inst.*, 2, 277-324.
- Watson, W. (1926): A Quartz-thread Vertical Force Magnetograph. *J. Sci. Instr.*, 3, 156-157.

柿岡の新標準磁気儀カスマー

柳原 一夫, 河村 謙, 佐野 幸三, 久保木忠夫

(地磁気観測所)

柿岡の地磁気標準観測のため新しい標準磁気儀が1972年8月に完成し、カスマーと名付けられた。主な構成要素は4台の光ポンピング磁力計、プロトン磁力計、角度測定器、計算処理装置などである。全体の装置は角度測定器を除いて自動的に動作させることができる。この標準磁気儀を使って地球磁場の各成分を 0.1γ の絶対精度で測定し、デジタル値として直ちにあらわすことができる。

4台の光ポンピング磁力計を使って全磁力、水平成分、鉛直成分、偏角の四つの成分を同時に測定するので、必要なときには 0.01 秒の時間分解能をうることもできる。またある成分の測定値を他の成分の測定値から合成したものと比較することによって、各磁力計の動作状態を監視したり精度を検討したりすることもできる。ある成分用の磁力計が故障した時には Alldredge の提唱した ASMO 方式によって補うようになっている。光ポンピング磁力計は精度は高いが、必ずしも絶対値精度がよいとはいえないので、プロトン磁力計と角度測定器によってその器械定数を検定する。角度測定器は新たに開発した測定原理を使った一種の磁気経緯儀で、地球磁場の偏角と伏角を角度1秒の精度で測定する。プロトン磁力計による全磁力測定と合わせて、地球磁場全成分の絶対値を与える。これによって校正された光ポンピング磁力計を使えば必要な時の地球磁場絶対値を直ちにうることができる。必要な計算処理は2台の超小型電子計算機で行なう。

1972年8月以降数カ月の試験結果では、 0.1γ の絶対精度をうる目標はほぼ達成されたように思われる。